THE UNIVERSITY of EDINBURGH

Edinburgh Research Explorer

Deglacial mesophotic reef demise on the Great Barrier Reef

Citation for published version:
Abbey, E, Webster, J, Braga, JC, Jacobsen, GE, Thorogood, G, Thomas, A, Camoin, G, Reimer, PJ & Potts, D 2013, 'Deglacial mesophotic reef demise on the Great Barrier Reef', *Palaeogeography, Palaeoclimatology, Palaeoecology*, vol. 392, pp. 473-494. https://doi.org/10.1016/j.palaeo.2013.09.032

Digital Object Identifier (DOI):
10.1016/j.palaeo.2013.09.032

Link:
Link to publication record in Edinburgh Research Explorer

Document Version:
Peer reviewed version

Published In:
Palaeogeography, Palaeoclimatology, Palaeoecology

General rights
Copyright for the publications made accessible via the Edinburgh Research Explorer is retained by the author(s) and / or other copyright owners and it is a condition of accessing these publications that users recognise and abide by the legal requirements associated with these rights.

Take down policy
The University of Edinburgh has made every reasonable effort to ensure that Edinburgh Research Explorer content complies with UK legislation. If you believe that the public display of this file breaches copyright please contact openaccess@ed.ac.uk providing details, and we will remove access to the work immediately and investigate your claim.

OPEN ACCESS

Download date: 06. May. 2023

*Manuscript
Click here to download Manuscript: Abbey_etal_fossil_meso_reefs_Pal3.docx Click here to view linked References

Deglacial mesophotic reef demise on the Great Barrier Reef

E. Abbey[1] J. M. Webster*[1], J.C. Braga[2], G.E. Jacobsen[3], G. Thorogood[4], A. L. Thomas[5, 6], G. Camoin[7], P. J. Reimer[8], D. C. Potts[9]

[1]Geocoastal Research Group, School of Geosciences, University of Sydney NSW 2006, Australia

[2]Departamento de Estratigrafia y Paleontologia, Universidad de Granada, Granada, Spain

[3]Institute for Environmental Research, Australian Nuclear Science and Technology Organisation, Locked Bag 2001, Kirrawee DC, NSW 2232, Australia

[4]Institute of Materials Engineering, Australian Nuclear Science and Technology Organisation, Locked Bag 2001, Kirrawee DC, NSW 2232, Australia

[5]University of Oxford, Department of Earth Sciences, Parks Road, Oxford, OX1 3PR, UK

[6]School of Geosciences, University of Edinburgh, West Mains Road, Edinburgh EH9 3JW, UK

[7]Aix-Marseille Université, CNRS, IRD, CEREGE UM34, Europôle Méditerranéen de l'Arbois, B.P. 80, F-13545 Aix-en-Provence CEDEX 4, France

[8]School of Geography, Archaeology and Palaeoecology (GAP), Queen's University Belfast, Belfast, BT7 1NN, Northern Ireland, UK

[9]Department of Earth and Evolutionary Biology, University of California, Santa Cruz, California 95604, USA

Corresponding author: Jody M. Webster, Geocoastal Research Group, School of Geosciences, The University of Sydney, NSW 2006, Australia; Tel: +02 9036 6538, Fax: +02 9351 0184, Email: jody.webster@sydney.edu.au

Abstract

Submerged reefs are important recorders of palaeo-environments and sea-level change, and provide the substrate for modern mesophotic (deep-water, light-dependent) coral communities. Mesophotic reefs are rarely, if ever, described from the fossil record and nothing is known of their long-term record on Great Barrier Reef (GBR). Sedimentological and palaeo-ecological analyses coupled with > 50 ^{14}C AMS and U-Th radiometric dates from dredged coral, algae and bryozoan specimens, recovered from depths of 45 to 130 m, reveal two distinct generations of fossil mesophotic coral community development on the submerged shelf edge reefs of the GBR. They occurred from 13-10 ka and 8 ka to present. We identified eleven sedimentary facies representing both autochthonous (in situ) and allochthonous (detrital) genesis, and their palaeo-environmental settings have been interpreted based on their sedimentological characteristics, biological assemblages, and the distribution of similar modern biota within the dredges. Facies on the shelf edge represent deep sedimentary environments, primarily forereef slope and open platform settings in palaeo-water depths of 45-95 m. Two coral-algal assemblages and one non-coral encruster assemblage were identified: 1) Massive and tabular corals including *Porites*, *Montipora* and faviids associated with Lithophylloids and minor Mastophoroids, 2) platy and encrusting corals including *Porites*, *Montipora* and *Pachyseris* associated with melobesioids and *Sporolithon,* and 3) Melobesiods and *Sporolithon* with acervulinids (foraminifera) and bryozoans. Based on their modern

occurrence on the GBR and Coral Sea and modern specimens collected in dredges, these are interpreted as representing palaeo-water depths of < 60 m, < 80-100 m and > 100 m respectively. The first mesophotic generation developed at modern depths of 85-130 m from 13-10.2 ka and exhibit a deepening succession of < 60 to >100 m palaeo-water depth through time. The second generation developed at depths of 45-70 m on the shelf edge from 7.8 ka to present and exhibit stable environmental conditions through time. The apparent hiatus that interrupted the mesophotic coral communities coincided with the timing of modern reef initiation on the GBR as well as a wide-spread, massive flux of siliciclastic sediments from the shelf to the basin. For the first time we have observed the response of mesophotic reef communities to millennial scale environmental perturbations, within the context of global sea-level rise and environmental changes.

Keywords: mesophotic reef, submerged reef, coralgal assemblages, radiocarbon dating

1. Introduction

Mesophotic reefs are light-dependent coralgal communities found on deep forereef slopes (ca. 40-100 m) along continental margins and oceanic islands (Lesser et al., 2009; Kahng et al., 2010). Their distribution is becoming increasingly well-known as they are the topic of much interest, thought to be refuges during past environmental calamities (summarised in Bongaerts et al., 2010). These communities are commonly composed of depth generalists found in shallow-water reefs (Bongaerts et al., 2010) and are thought to be the source for a new reef generation once poor conditions at the surface have passed. However, the genetic and ecological link between mesophotic communities and shallow-water reefs is unclear (Van Oppen et

al., 2011). The mesophotic reefs' ecological role in regenerating shallow-water reefs following modern disturbances is still unclear (Bongaerts et al., 2010), and their presence in the fossil record and response to Quaternary sea-level and climate fluctuations is poorly documented compared with their shallow counterparts.

Sea-levels dropped to a maximum level of about 125 m during the Last Glacial Maximum (LGM) (Yokoyama et al., 2001; Peltier, 2002; Peltier and Fairbanks, 2006), and evidence for shallow-water reef colonisation on deep island flanks and continental shelf edges during the deglacial sea-level rise can be found in the South Pacific (Salvat et al., 1985; Camoin et al., 2006; Cabioch et al., 2008; Flamand et al., 2008), Hawaii (Grigg et al., 2002; Webster et al., 2004; Faichney et al., 2009), the Caribbean Sea (Macintyre, 1967; Adey et al., 1977; Macintyre et al., 1991; Toscano and Lundberg, 1999; Blanchon et al., 2002), the Indian Ocean (Siddiquie, 1975; Wagle et al., 1994; Vora et al., 1996; Dullo et al., 1998; Rao et al., 2003; Camoin et al., 2004; Fürstenau et al., 2010) and Australia (Harris and Davies, 1989; Harris et al., 2004; Beaman et al., 2008; Woodroffe et al., 2010; Abbey et al., 2011a). Indications of rapid pulses in sea-level rise during the last deglaciation (meltwater pulses) have been identified in the submerged reef and coastal sequences in the Caribbean and the Indo-Pacific (Fairbanks, 1989; Bard et al., 1996; Hanebuth et al., 2000; Webster et al., 2004; Fairbanks et al., 2005; Camoin et al., 2012; Deschamps et al., 2012), with coral reefs responding to rapidly changing environmental conditions via a combination of community transitions, and/or complete demise and backstepping.

The causes for shallow-water reef demise have increasingly been studied in both the modern (e.g., Eakin et al., 2010) and the fossil records (e.g., Montaggioni, 2005;

Blanchon, 2011). However, the causes and occurrence of modern mesophotic reef demise are relatively unknown (Smith et al., 2010). Mesophotic coral communities are similar in composition to their shallow-water counterparts (Bongaerts et al., 2010; Bridge et al., 2012), and as such are difficult to differentiate in fossil coral cores without the aid of multi-taxa reconstructions and precise radiometric dating. Mesophotic reefs also tend to have slow accretion rates (Grigg, 2006) and produce only a thin veneer of coral growth (e.g., Jarrett et al., 2005; Abbey et al., 2011b) and as such, there is limited potential to investigate fossil mesophotic reef death in vertical drilled sequences alone. Despite these limitations, as the final stage of reef growth prior to drowning, fossil mesophotic reefs have the potential to provide valuable information about conditions during sea-level rise, as well as better constraining mesophotic tolerances.

Due to its wide (50-150 km), mostly gently-sloping continental shelf reaching depths of >100 m (Hopley et al., 2007), the Great Barrier Reef (GBR) offers an excellent opportunity to study fossil mesophotic communities and their response to sea-level rise and palaeo-environmental changes. Modern mesophotic communities are found on submerged Pleistocene reefs to depths of 75 m (Bridge et al., 2010; Bridge et al., 2011a; Bridge et al., 2011b), and provide a robust foundation for environmental reconstruction through direct comparisons of the fossil communities to the modern.

Despite intensive study of the Holocene growth history of the modern GBR (see Hopley et al., 2007 for a comprehensive review), little is known of the submerged reefs found at the shelf edge. Submerged geomorphological features at depths of 50-130 m are interpreted to be the result of widespread reef growth during the deglaciation and previous periods (Harris and Davies, 1989; Beaman et al., 2008;

117 Abbey et al., 2011a), but ecological and chronological information is sparse (Veeh
118 and Veevers, 1970; Yokoyama et al., 2000; Davies et al., 2004). Prior to this study,
119 only two corals have been recovered from these deep slopes, both in the southern
120 GBR; a *Galaxea clavus* was recovered from 175 m depth and dated to 17.0 ka
121 (Veeh and Veevers, 1970; Yokoyama et al., 2000), and an encrusting Acroporid was
122 recovered from 90-110 m and dated to 9.1 ka (Davies et al., 2004). However, a
123 recent program of offshore drilling on the shelf edge has targeted these submerged
124 geomorphological features, and preliminary results confirm the underlying structure
125 is composed of a combination of mainly shallow water coralgal-microbial framework
126 and detrital facies that developed since the LGM (Webster et al., 2011).

127 Therefore, the deeper regions of the GBR shelf edge may provide not only important
128 information about shallow fossil reefs but also new insights into the fossil mesophotic
129 communities, their palaeo-environments and the timing and causes of their demise.
130 Our study is based on samples and data collected on a 2007 cruise on the RV
131 *Southern Surveyor* that investigated the geomorphology, fossil coral communities
132 and modern benthic habitats preserved on the outer shelf of the GBR (Webster et
133 al., 2008). The specific objectives of our study are; (1) to describe the ecological and
134 sedimentological characteristics of the fossil mesophotic communities and their
135 palaeo-environmental significance; (2) constrain the timing of mesophotic reef turnoff
136 and assess the cause of death during the last deglaciation; and (3) discuss the
137 implications of these findings for understanding the environmental thresholds of
138 these deep-water communities.

2. Location and methods

The GBR extends from ca. 10° to 24°S along Australia's eastern continental shelf. Conditions are oligotrophic on the shelf edge where reefs grade from a nearly continuous barrier in the north to isolated platforms in the central region (Hopley et al., 2007). Shelf edge reefs are buffered from terrestrial influences due to their great distance from the shore (King et al., 2001; Brinkman et al., 2002). Four widely-spaced shelf edge sites on the GBR were selected for this study, including near Ribbon Reef 5, near Noggin Pass, near Viper Reef and near Hydrographers Passage (Figs. 1 and 2). Abbey et al. (2011a) conducted a detailed study of shelf geomorphology at these four sites, and identified drowned reef features including fringing reefs, patch reefs, an outer barrier reef and an inner barrier reef. Many of these features were dredged, including the following:

1. **Continental slope**: the slope seaward of the shelf break.
2. **Shelf break**: the inflection point demarking the continental slope from the continental shelf.
3. **Terraces**: flat, horizontal or sub-horizontal features bound on their landward and seaward margins by more steeply dipping sea bed.
4. **Pinnacles**: high relief, steep sided outcrops, generally circular to oval in shape and less than 100 m in diameter.
5. **Barrier reefs**: high relief outcrops with extensive linear continuity. They may be flat-topped or formed by closely-spaced or joined pinnacles.

[FIGURE 1]

[FIGURE 2]

2.1. Dredging

Samples were recovered using a benthic sled, designed to recover the top layer of the substrate as it was towed over a distance of 50-250 m at each sampling site. Twenty-two dredges were recovered from between 46 m and 173 m (Table 1) with depth ranges estimated using a combination of shipboard GPS and 5 m pixel cell size bathymetric models (Bridge et al., 2010; Abbey et al., 2011a; Bridge et al., 2011a). Depth errors were minimized (5-10 m) by dredging parallel to the isobath in most cases (Figure 2).

[FIGURE 2]

[TABLE 1]

2.2. Biota, bio-litho facies and environmental characterisation

Samples larger than ca. 50 mm in diameter were halved along their long axis and used for analyses and those smaller than 50 mm were not included. The cut surfaces of more than 900 selected samples were used to assess the facies, fossil assemblages and internal bioerosion.

Modern biota was identified by the presence of live tissue and recent biota by preservation of fine-scale surface ornamentation but lacking tissue and/or a modern (< 500 years) radiometric age. The degree of bioerosion was estimated visually (Flügel, 2009) as a percentage of the cut surface area affected by voids created by boring organisms. Each sample was classified using Wright's (1992) revised version of Dunham's (1962) and Klovan and Embry's (1971) classifications. Samples were considered in situ on the basis of a freshly broken basal surface lacking any encrusting biota. Additional factors taken into account include the orientation of

185 geopetals and the location of staining relative to the upper surface indicated by the
186 biota (e.g. corallites). Those samples exhibiting rounding, no freshly broken basal
187 surface or encrustations on a broken basal surface were interpreted to have been
188 reworked and transported.

189 The taxonomy and growth form of biota found within the samples were recorded,
190 especially for corals, coralline algae, bryozoans and encrusting foraminifera.
191 Exposed corallites and skeletal cross sections were used for identification of corals
192 in conjunction with taxonomic guides (Veron et al., 1977; Veron and Pichon, 1979;
193 Veron and Pichon, 1982; Veron and Wallace, 1984; Veron, 1986; Veron, 2000).
194 Seventy-four thin sections were used for the identification of coralline algae and
195 encrusting foraminifera. In cut specimens, the maximum thickness of algal crusts
196 was measured and the volumetric ratio of algae to foraminifera was estimated.
197 Selected bryozoans were identified by zooecial chambers using a scanning electron
198 microscope. The percent of the limestones' surface area encrusted was estimated
199 visually; epibiont identifications were made; and their relative abundance was
200 recorded on a six point scale using the terms "absent", "rare", "occasional",
201 "frequent", "common" and "abundant". Models of vertical succession were
202 constructed using a stratigraphic analysis of the fossil assemblage compositions,
203 and placed within an absolute temporal context using radiometric dating.

204 **2.2. Radiometric dating**

205 Radiocarbon dating by accelerator mass spectrometry (AMS) was the preferred
206 method due to the small sample size necessary and the type of fossil to be dated.
207 Four coral samples (including one replicate to total five measurements) were
208 selected for U-Th dating to determine the local ΔR. In situ samples were

preferentially selected, but the primary objective was to date a range of biota, including corals, coralline algae (geniculate and non-geniculate) and bryozoans. Pre-treatment for AMS was rigorous due to the degraded state of many of the samples, and the calcite content determined by XRD prior to preparing samples for AMS analysis.

2.2.1 AMS Radiocarbon measurement

2.2.1.1 OZ- Samples

Sub-samples were extracted using a Dremel drill with a diamond wheel. Unlithified infill was removed in an ultrasonic bath using Milli-RO water and then organic matter was removed by treating with 10% H_2O_2 for 24 hours. Etching with a dilute solution of HCl (0.125 N) removed 20-80% of each sub-sample to reduce secondary aragonite and high Mg-calcite. Coral samples were analysed for secondary calcite content before preparing samples for AMS analysis (section 2.2.1.1.1). Samples 5-20 mg were then treated with H_3PO_4 (85%) at 60˚C overnight to release CO_2, which was then converted to graphite by reduction with H_2 over an iron catalyst at 600˚C (Hua et al., 2001). The graphite target was then analysed by AMS using a HVEE 2MV tandem accelerator at ANSTO. The measurements were normalised to an oxalic acid standard, corrected for background using IAEC C1 Carrera marble (Rozanski et al., 1992) and for fractionation (using $\delta^{13}C$ measured separately on a Micromass IsoPrime IRMS with Elemetar Elemental Analyser) to give the conventional radiocarbon age (Fink et al., 2004).

2.2.1.1.1 XRD Analysis

All pre-treated coral samples were powdered for X-ray diffraction (XRD) to quantify contamination and possible calcite recrystallization. The measurements were carried out using a PANalytical X'Pert Pro Diffractometer with Cu Kα radiation and collected over a 2θ range of 5° to 80°. About 50 mg of powdered coral was used for each test and aragonite standards with 0.1, 0.5, 2.0, 10.0 and 20.0% calcite were used for calibration. To test the efficiency of calcite removal, both pre-treated and untreated material from the same sample was analysed (sample OZL402). Calcite was reduced from 1.0% to 0.2% after 78% dissolution. All scleractinian corals comprise < 2% calcite after etching, with most of the samples < 1% calcite.

2.2.1.2 UBA- Samples

Coral samples were pre-treated following the method described in Burr et al. (2004). Calcite content was determined using XRD, to ensure samples contain <1% calcite. A small slab of coral was removed using a Dremel, and washed several times in Milli-Q water using ultrasonication, then dried. Approximately 17 mg of the cleaned coral was transferred to a septa sealed vial and an appropriate amount of ~0.1 N HCl added to etch 50-60% of the sample, and allowed to react for 1-2 days. The remaining coral was washed several times with Milli-Q water then placed in a vial under vacuum until dry. The coral was reacted with 0.5 ml of H_3PO_4 (80%) at 90^{o}C until all the coral had dissolved. The carbon dioxide was transferred to the graphitisation reactor and graphitised in the presence of an iron catalyst at 560 ºC for a maximum of 4 hours according to the Bosch-Manning Hydrogen Reduction Method (Manning and Reid, 1977; Vogel et al., 1984).

The $^{14}C/^{12}C$ and $^{13}C/^{12}C$ ratios were measured by accelerator mass spectrometry (AMS) on a 0.5 MV National Electostatics Corporation compact accelerator, at the

14CHRONO Centre, Queen's University Belfast, together with Icelandic spar samples for the background (blank) and TIRI turbidite secondary standards (Scott, 2006). The sample $^{14}C/^{12}C$ ratio was background corrected and normalised to the HOXII standard (SRM 4990C; National Institute of Standards and Technology).

For all radiocarbon samples the ^{14}C age and 1 sigma error were calculated using the Libby half-life of 5568 yr following the conventions of Stuiver and Polach (1977). The ages were corrected for isotope fractionation using the AMS-measured $\delta^{13}C$, which accounts for both natural and machine fractionation. Conventional radiocarbon ages were calibrated using Calib rev.6.0.1 (Stuiver and Reimer, 1993) using the Marine 09.14c calibration curve (Hughen et al., 2004; Reimer et al., 2009), applying a locally derived regional marine correction (ΔR) of 8±6 years (Druffel and Griffin, 1993; Druffel and Griffin, 1999). Paired measurements of U-Th and radiocarbon on four corals measured in this study suggest that ΔR may have been more variable. This extra variability will introduce some additional uncertainty to the calibrated ages for a few hundred years (ca. 200), but for the purposes of this study are not significant. Radiocarbon ages, calibrated ages and % calcite are reported in Table 8.

2.2.2 U-Th Dating

U-Th dating samples were subsampled with a diamond cutting wheel to avoid visible signs of alteration and bioerosion. Sample pre-treatment consisted of ultrasonication in 18 MΩcm water to remove particulate contaminants. Sub-samples of 0.2-0.5 g were spiked with a mixed ^{229}Th-^{236}U tracer solution (Robinson et al., 2004) and dissolved with HNO_3. Sample/spike equilibration was achieved by refluxing in aqua regia, drying down and dissolving twice in 15 N HNO_3. Purification of U and Th was performed by anion exchange chromatography following a procedure adapted from

Edwards et al., (1986). Mass spectrometric measurement of U and Th isotope ratios was by a Nu Instruments MC-ICP-MS, with minor isotopes ^{234}U, ^{230}Th and ^{229}Th collected in an ion counter and all other beams measured in Faraday collectors. Instrumental biases were corrected using a standard-sample-standard bracketing approach with CRM-145 bracketing U samples and an in-house Th isotope standard for Th samples (Mason and Henderson, 2010). Isotope ratios are presented in Table 2 and U-Th ages are presented in Table 9.

[TABLE 2]

3. Results

3.1. Taxonomy, growth form and distribution of biota

The primary biological components within samples include corals, encrusting red coralline algae (CCA), bryozoans and encrusting foraminifera. Secondary fossil components includes calcareous green algae and benthic foraminifera. Living and recent biota were identified through the presence of soft tissue (corals reported by Bridge et al., 2011b), excellent preservation of surface ornamentation and/or a modern (< 500 years) radiometric age. Most samples are moderately encrusted (50% or more) with two or more epibionts classified as ‘common’ or ‘frequent’ within each dredge (see Fig. 6). Specimens of live encrusting coralline algae (CCA) were obtained from dredges ranging in depth from 45-130 m, and live corals were recovered from dredges ranging in depth from 45-100 m (Fig. 3).

[FIGURE 3]

In total, four species, fourteen genera and seven Scleractinian families were identified and one unidentified family of Octocorallia. Eleven species, ten genera and

four families of red algae were recognised and one green algae genus. Two genera of encrusting foraminifera and one genus of thick encrusting and large platy bryozoans were identified (Table 3).

[TABLE 3]

Porites and *Montipora* are the most abundant corals and agariciids are common (Table 3). Coral morphology is dominated by the encrusting, platy, tabular and massive (domal) growth forms with rare branching corals (Fig. 4). Modern corals with encrusting or platy morphology have the widest depth range, and are found as deep as 100 m, but more commonly to a maximum of 80 m (Bridge et al., 2010; Bridge et al., 2011b and data herein). Massive and tabular corals are more restricted and found to depths of 60 m.

[FIGURE 4]

Fossil coral diversity is similar between sites with some minor variability in the distribution of the less-common corals: *Galaxea* are absent from Viper Reef, *Cyphastrea* are absent from Noggin Pass, *Goniopora* are absent from Hydrographers Passage, and *Echinopora* are only present at Noggin Pass (Table 4). Corals on the outer reef and upper shelf (ca. 45-60 m) had the highest taxonomic and morphologic diversity (Table 4), and diversity and abundance decrease with increasing depth.

[TABLE 4]

Modern algal crusts are dominated by the mastophoroid and lithophylloid sub-families (e.g., *Hydrolithon*, *Neogoniolithon, Lithophyllum*) and the melobesioid sub-family (e.g., *Lithothamnion*, *Mesophyllum*) with common *Sporolithon* and

325 *Peyssonnelia* (Fig. 5). Similar to corals, CCA also exhibit depth zonation, with the
326 mastophoroids/lithophylloids found to about 55-60 m, and melobesioids found to 95
327 m or deeper (Fig. 3). CCA are most commonly found at the outer barrier reef, and
328 decrease in volume with increasing depth (Fig. 6).

329 [FIGURE 5]

330 [FIGURE 6]

331 Acervulinids (e.g., *Acervulinid* sp. and *Gypsina* sp.) are not depth restricted but
332 become the dominant non-coral encrusters with increasing depth. Modern encrusting
333 (thin and lacey) bryozoans were not identified taxonomically, but they are most
334 commonly found on the shelf break (Fig. 6). A thick (> 2 cm) platy growth
335 morphology was also present on the shelf edge, upper slope and shelf break and
336 was identified as *Celleporaria* sp.

337 Based on the taxonomic and morphologic observations of the modern biota, three
338 distinct assemblages in relation to depth can be summarised (Table 5).

339 1. **Massive/tabular corals:** Similar to previously observed mesophotic corals
340 (e.g., Reed, 1985; Bak et al., 2005; Bridge et al., 2010), these corals exhibit a
341 marked morphologic change in the transition from shallow to deep, whereby
342 corals assume a flatter morphology at depths greater than 30 m. Corals
343 between 45-60 m are primarily massive or tabular (flat and thick), especially
344 *Porites*, *Montipora* and faviids. The CCA within this depth range are
345 dominated by lithophylloids and secondary or minor mastophoroids.
346 2. **Platy/encrusting corals:** At depths greater than 60 m the flattened massive
347 corals are replaced by much thinner (< 2 cm), platy and encrusting

morphologies, especially *Porites*, *Montipora* and agariciids. CCA are dominated by melobesioids and *Sporolithon*.

3. **Non-coral encrusters:** At depths greater than 100 m, biota include a range of octocorals (Bridge et al., 2011b) and algal-foraminiferal communities. CCA include *Peyssonnelia* and *Sporolithon* to the exclusion of all lithophylloids and mastophoroids.

[TABLE 5]

3.2. Bio-litho facies and environmental interpretation

Using sedimentary and textural observations in conjunction with fossil assemblages, six in situ (autochthonous) facies and five detrital (allochthonous) sedimentary facies have been identified (see Table 6 for detailed descriptions). Facies can be grouped into three primary categories based on their genesis which include: 1) boundstones (including six sub-facies, Table 6; Fig. 7D), indurated boundstones (Fig. 7A) and isolated colonies; 2) macroids and rhodoliths (Fig. 7C); and 3) allochthonous grainstones, floatstones, rudstones, shellstones and calcimudstones (Fig. 7B). The environmental interpretations of the facies are based on their mode of genesis, characteristic fossil components and the modern distribution of similar facies across the shelf (see Table 7 for details).

[FIGURE 7]

[TABLE 6]

[TABLE 7]

The composition and genesis of bio-litho facies is a useful indicator of palaeo-environment and water depth when modern analogues can be identified. The use of analogous coral and coralline algae distribution for palaeo-water depth reconstructions is a well-established methodology (Lighty et al., 1982; Adey, 1986; Pirazzoli and Montaggioni, 1988; Cabioch et al., 1999).

3.2.1. Boundstones and isolated colonies

Boundstones and isolated colonies have the most diverse composition of the bio-litho facies and have a widespread distribution across the shelf edge. They are most commonly found on the upper slope, shelf break or the outer barrier reef (Fig. 8). The interpretation of the coral/coralgal boundstone and isolated colony facies is based on the distribution of the modern coral and algae analogues.

[FIGURE 8]

Coral and coralgal boundstones and isolated colonies generally comprise one of the coralgal assemblages identified in the modern biota (Table 5). Coralgal boundstones are considered photophilic, as each component is dependent upon irradiance for metabolism. As such, all coralgal boundstones have an interpreted depth range of < 60 m, and < 80-100 m which is consistent with the observed photic zone (Hopley et al., 2007) and their modern distribution (Table 5). When boundstones comprise a coralgal assemblage and components, such as foraminifera and bryozoans, the interpretation is based on the order of overgrowth and vertical succession discussed in more detail below.

Modern algal-foraminiferal boundstones were not found to be depth-restricted (within the 130 m depth sampling range) and therefore provide little depth constraint for the

392 fossil assemblage. However, acervulinids are poor competitors for space and where
393 they dominate, it is usually due to the reduction of CCA in low-light and cryptic
394 environments (Perrin, 1992; Flamand et al., 2008). Modern platy bryozoans were not
395 recovered in dredges and therefore their modern distribution on the GBR is
396 unconstrained. However, *Celleporaria* sp. are found along the southern margin of
397 Western Australia in low-energy, mesotrophic environments with moderate
398 sedimentation (Hageman et al., 2003). Their development is especially supported
399 during low sea-levels when upwelling and lower surface temperatures favour a well-
400 mixed water column.

401 **3.2.2. Indurated boundstones**

402 The indurated boundstones generally have little identifiable biota and none that is
403 modern, but are characterised by dense, lithified pelagic or hemipelagic sediments
404 within the skeletal interstices, borings and between algal and foraminiferal crusts
405 (Fig. 7A). Indurated boundstones are found on the shelf break at depths of 100 m or
406 more (Fig. 8). These sediments, combined with the algal and foraminiferal crusts,
407 indicate deep conditions with limited terrigenous input (Flügel, 2009) (assumed by
408 the pelagic origin of sediments) and occur on deep, open platform settings.

409 **3.2.3. Macroids and rhodoliths**

410 These coated structures form through successive episodes of encrustation and
411 repeated repositioning or turning, as they are unattached to the seabed. This
412 movement can be a result of near-bottom currents, bioturbation or a combination of
413 the two (Bosence, 1983; Harris et al., 1996). Macroids and rhodoliths are not
414 commonly a dominant facies across the shelf edge within this study, but are highly
415 concentrated at Viper Reef on the upper shelf from 55-70 m (Fig. 8) where

substrates are probably more mobile. Rhodoliths have also been observed on the Queensland shelf to depths of ca. 120 m, but are more commonly found down to about 90-100 m (Harris et al., 1996; Marshall et al., 1998; Lund et al., 2000). The algal components of the macroids (*Lithothamnion*, *M. funafutiense* and *Lithoporella*, Table 6) identified here are similar to those found within rhodoliths.

3.3 Vertical biologic succession

Small-scale, local biological succession can be observed in the form of encrusting overgrowths within a single sample, usually a boundstone. The patterns of vertical succession are a useful record of environmental and ecological change, especially in instances where radiometric dating is unavailable. Three distinct overgrowth patterns are common across the shelf and can be characterised by their photophilic or cryptic biota and transitions from one into another (Fig. 9). Using these successions, the ecological trajectory can be used to better understand changing environments (e.g., deepening or changing water clarity).

[FIGURE 9]

In a stable photophilic succession, corals are overgrown by other corals or thick CCA. In a succession from photophilic to cryptic, corals are overgrown by bryozoans or thick acervulinids, and in a stable cryptic succession, CCA and acervulinids are interlayered. These successions are distributed evenly across each of the four sites, but vary with depth. In the very deepest dredge at 159-172 m, CCA are intercalated with peloidal and hemipelagic infill in a stable cryptic succession. On the upper slope from about 100-130 m, all three patterns of vertical succession are apparent, and on the shelf break from 100-110 m, CCA are overlain by dark, indurated pelagic sediments in a stable cryptic succession. On the terrace top and rim from 85-95 m,

successions of stable photophilic corals and CCA as well as photophilic to cryptic corals encrusted by thick bryozoans are present. On the upper shelf and outer barrier reef from 45-60 m, corals and CCA alternate in thick layers for many generations in a stable photophilic succession.

3.4. Chronology

Radiocarbon and U-Th dating from fifty-four specimens, including corals, CCA and bryozoans, reveal the fossil reef components distributed across the shelf edge range in age from about 16 ka to modern, with ages clustering mainly between 9-13 ka, 5-8 ka and 0-2 ka (Tables 8 and 9). The ages within a single dredge can vary by up to 5.5 ky, but are usually within 2-3 ky (Fig. 10).

[FIGURE 10]

[TABLE 8]

[TABLE 9]

Several corals underwent dual radiocarbon-uranium-series dating or replicate radiocarbon dating to ensure reproducibility, and validate the reservoir correction. All replicate radiocarbon ages are consistent within a 2σ error. One dual radiocarbon-uranium series coral date varies by more than 2σ, though the difference is not significant for the purposes of this study. Most chronology was performed on the boundstone facies, with some dates from detrital facies as well. Components that were radiometrically dated (directly dated) and those components observed within the same boundstone (indirectly dated) include corals, bryozoans, acervulinids and CCA.

462 CCA are the oldest fossil components directly or indirectly dated, and are also the
463 most persistent, spanning the longest time period. They occurred within indurated
464 boundstones from 16-14 ka on the submarine landslide at 159-172 m and then within
465 coral-algal boundstones (indirectly dated) as well as within foraminiferal-algal
466 boundstones (directly dated) from 13-10.1 ka at 95-130 m. From 9.5-9.1 ka algae
467 again occurred within indurated boundstones at 100 m. The longest gap in direct or
468 indirect dating occurs from 9.1-7.8 ka. From 7.8 ka to present, CCA have grown
469 within algal and coral-algal boundstones at > 60-80 and 95 m, and within indurated
470 boundstones at 105 m.

471 Corals within coral and coral-algal boundstones occurred on the shelf from 13-10.1
472 ka at 95-130 m. Corals had both the earliest and latest occurrence at Hydrographers
473 Passage, spanning the entire range from 13-10.1 ka. At Noggin Pass, coral
474 presence overlapped with that at Hydrographers Passage 11.3-10.2, and at Viper
475 Reef from 12.3-11.1 ka. No corals were dated (directly or indirectly through
476 overgrowths) from 10.1-7.8 ka at any depth across the shelf, but were again within
477 coral-algal boundstones at 7.8 ka at 60 m. Following this apparent hiatus, some
478 corals developed at greater depths of 95-100 m from 7.8 to present, but most were
479 primarily within the depth range of the modern mesophotic communities at < 80 m.

480 Detrital facies and large platy bryozoans were rarely dated. The earliest occurrence
481 of bryozoan boundstones was 13 ka at 95 m and they were present through to 9.5 ka
482 to depths of 130 m. These fossil platy bryozoans were found primarily at
483 Hydrographers Passage and no modern equivalents were observed following the
484 hiatus. Detrital floatstones and rudstones comprising *Halimeda* plates were dated to
485 11.8-11.0 ka at depths of 100-130 m, and again at 7.2 ka at 95 m.

4. Discussion

The sedimentology, palaeoecology and radiometric data from the continental margin of the GBR indicates a more widespread, diverse and temporally dynamic fossil mesophotic reef system than previously recognised. These communities persisted at depths which up until now have been poorly constrained in fossil mesophotic systems, and as such they provide a unique perspective on marginal habitats during periods of lower sea-level and rise. Based on a synthesis of geomorphologic, sedimentologic and palaeoecologic data, we have reconstructed the range of depositional environments across the shelf edge. Combined with a comprehensive chronologic framework, we can now place the development of these fossil mesophotic communities within the context of sea-level rise and environmental perturbations, to better understand their environmental thresholds.

4.1. Mesophotic reef growth and succession across the shelf edge

Both the modern and fossil mesophotic corals and CCA are consistent with other deep-water observations in the GBR (Marshall et al., 1998; Lund et al., 2000; Davies et al., 2004; Bridge et al., 2010; Bridge et al., 2011a; Bridge et al., 2011b). The live corals that were recovered from depths of 45-80 m are all known as ‘depth generalists’ (reviewed in Bongaerts et al., 2010) and are commonly found in both shallow-water reefs (0-20 m) and mesophotic communities (30 to ≥ 60 m). Such modern mesophotic reefs extend to 100 m at Myrmidon Reef (Hopley et al., 2007) and in the nearby Coral Sea (Bongaerts et al., 2011). Within the study area, live corals are found to 75 m, and very sparse coral coverage even extends to 75-100 m (Bridge et al., 2010; Bridge et al., 2011a; Bridge et al., 2011b). Some of the most common corals within these modern mesophotic communities include *Acropora*,

510 *Montipora*, agariciids (e.g., *Pachyseris)*, *Galaxea*, *Goniopora* and *Porites*. Similarly,
511 the living coralline algae, including the abundant melobesioids and *Sporolithon* are
512 common in cryptic and mesophotic environments extending to depths greater than
513 100 m (Adey, 1986; Minnery, 1990; Iryu et al., 1995; Lund et al., 2000; Braga and
514 Aguirre, 2004).

515 **4.1.1. Shelf-wide patterns of response and succession**

516 By combining patterns of vertical biological succession within the samples with the
517 radiometrically dated coralgal assemblages, three broad trends in water-depth and
518 sea-level rise are present across the shelf edge. The first pattern is characterised by
519 a stable photophilic succession of corals from the massive/tabular coralgal
520 assemblage (i.e. corals and CCA interlayered, Fig. 9A). The coralgal assemblage
521 (Table 5) present in this succession is restricted to 60 m based on the modern
522 distribution (Fig. 3). When this assemblage persists as a succession, it is indicative
523 of relatively stable mesophotic environments within 60 m water depth.

524 The second pattern is characterised by the succession of photophilic corals of the
525 platy and encrusting coralgal assemblage (Table 5) into more cryptic biota (i.e.
526 corals and CCA, then acervulinids or bryozoan, Fig. 9B). This succession from
527 photophilic to cryptic suggests progressively deepening environments, but the
528 mesophotic coralgal assemblage indicates an initial depth that is still within the
529 photic zone. Palaeo-water depths based on the assemblage interpretation are most
530 likely greater than 60 m in order to exclude the massive corals, and probably 80-100
531 m.

532 The third pattern consists of the stable cryptic succession of the non-coral encruster
533 assemblage (i.e. CCA, acervulinids and bryozoans, Fig. 9C). The lack of corals

indicates sea-level rise has submerged surfaces to depths greater than 100 m. This cryptic succession, comprising low-light tolerant CCA and fully heterotrophic biota (acervulinids and bryozoans, Table 5), has also been found on the deep forereef slopes of New Caledonia in water depths of 110-160 m (Flamand et al., 2008).

4.1.1.1. Response and succession at 100-130 m

Samples at a modern depth range of 100-130 m exhibit all three patterns of vertical succession, including mesophotic coral community development in stable conditions, a transition into a cryptic environment, and the sustained development of cryptic biota after deep submergence (Fig. 9). Radiometric dating (Table 8), palaeo-environmental interpretations (Table 5), and reconstructed sea-level (see Yokoyama et al., 2006 for a discussion on possible biases) are consistent with mesophotic and mesophotic-cryptic community development in palaeo-water depths of < 60-70 m from 13-10 ka (Fig. 11). From 10 ka to the present, exclusively cryptic communities had replaced the coral assemblages. The palaeo-environmental interpretation of the cryptic biota (Table 5), similar observations of cryptic biota on New Caledonia (Flamand et al., 2008) and known sea-level, are consistent with this community developing at depths of 80-130 m during the last 10 ka.

[FIGURE 11]

4.1.1.2. Response and succession at 85-95 m

At modern depths of 85-95 m only two patterns of succession within limestones were observed. A stable mesophotic community developed in palaeo-water depths of < 60 m from 12-10 ka. Based on the coralgal assemblages, palaeo-water depths exceeded 60 m by 10 ka. No corals are recorded again at this depth until 5.5 ka,

where communities shifted into the transitional mesophotic-cryptic community dominated by platy and encrusting corals (Fig. 11).

4.1.1.3. Response and succession at 45-60 m

At modern depths of 45-60 m, steady photophilic succession (Fig. 9) is coupled with the massive coralgal assemblage (Table 5).The earliest age of mesophotic coral development for this surface is 7.8 ka, which is consistent with the palaeo-water depth interpretation of the assemblage and known sea-level during the last ca. 8 ka (Fig. 11, Table 5). This massive coralgal assemblage continues to be widespread across the shelf within the modern mesophotic communities (Bridge et al., 2010; Bridge et al., 2011a; Bridge et al., 2011b).

4.2. Mesophotic community generations

Based on observations of community composition, development, vertical succession patterns and chronology, we have identified two distinct generations of mesophotic coral growth across the shelf. The first generation began by 13 ka and ended at 11-10.2 ka, characterised by the shift from mesophotic coralgal assemblages into transitional or wholly cryptic non-coral assemblages at depths of 85-130 m (Fig. 12) at Hydrographers Passage, Noggin Pass and Viper Reef. A cursory analysis of another coral record from the GBR also shows indications of a hiatus ca. 10 ka. Drill cores from IODP Expedition 325 penetrated the dredged surfaces at depths ranging from ca. 50-130 m. Sixty-seven corals from eighteen cores drilled at three of the four study sites have been dated using U-Th and ^{14}C AMS (Webster et al., 2011), and corals within 1 m of the seafloor range in age from ca. 13.5-9.7 ka (ages from unconsolidated facies were excluded).

580 [FIGURE 12]

581 Across the shelf and indicated by both dredges and IODP drill cores, a 2 ky hiatus in
582 mesophotic coral growth occurred between 10.2 and 7.8 ka when communities were
583 dominated by the deep non-coral, encrusting algae-foraminiferal assemblage. The
584 hiatus ended with the development of a second mesophotic coral generation at 7.8
585 ka, where similar coral communities to those of the first mesophotic generation
586 reformed upslope at depths of 45-95 m.

587 Shallow-water reef generations, (sensu Montaggioni, 2005, also observed in
588 Marquesas Islands, French Polynesia by Cabioch et al., 2008) are characterised by
589 periods of reef accretion punctuated by major growth hiatuses. The causes of the
590 shallow hiatuses have been correlated with meltwater pulses that would have
591 induced reef drowning, including the terminal LGM ca. 19 ka (Lambeck et al., 2000;
592 Yokoyama et al., 2001), MWP-1A ca. 13.8-14.7 ka (Fairbanks, 1989; Bard et al.,
593 1996; Hanebuth et al., 2000; Webster et al., 2004; Fairbanks et al., 2005;
594 Deschamps et al., 2012) and MWP-1B ca. 10-11 ka (Fairbanks, 1989; Bard et al.,
595 1990; Fairbanks, 1990; Bard et al., 1996). These mesophotic generations are distinct
596 from their shallow-water counterparts in that the timing of the hiatus at 10-8 ka is not
597 closely correlated with a known meltwater pulse (Fig. 13). Instead, the end of the first
598 mesophotic generation about 10 ka is coincident with the initiation of modern reefs of
599 the GBR shelf (Fig. 13) and the Gulf of Carpentaria (Harris et al., 2008), all of which
600 developed on surfaces ca. 20-30 m. The large spatial scale of this reef demise/reef
601 turn on event suggests an equally large-scale environmental change or perturbation.

602 [FIGURE 13]

4.3. Causes for mesophotic coral demise

Causes for reef demise are varied and poorly documented for mesophotic coral communities. However, a recent study (Smith et al., 2010) shows that these marginal habitats can experience wide-scale mortality events while nearby shallow-water reefs are left untouched, termed 'cryptic mortality'. In the GBR, fossil mesophotic and drilled coral communities ceased growth across a wide depth range spanning 60 m from 45-105 m depth in palaeo-water depths of 30-70 m. This death occurred within 100 years at two of the four sites, and within 1000 years when all three sites containing fossil communities are considered (Noggin Reef, Viper Reef, Hydrographers Pass). Due to the widespread nature of the hiatus on the GBR, the cause of coral demise is likely related to a regional change in the environment such as sea-level rise and/or increasing sediment flux.

Shallow reef drowning and backstepping has been recognised in the Caribbean as clear indicators of a jump in sea-level (Blanchon et al., 2002). In the depauperate Caribbean communities, small changes in sea-level have a more significant effect on the overall community structure, which might explain why similar instances of reef drowning and backstepping have not been recorded in the highly diverse Pacific coral reefs (Blanchon, 2011) over this same period. Mesophotic coral communities of the GBR may be more susceptible to perturbations, as they are relatively depauperate and expected to have only ca. 80-90 species represented (Bridge et al., 2011b) compared to 300+ living in the shallow environments. Mesophotic corals living at their maximum depth range may also be intrinsically more susceptible to mortality (Anthony and Connolly, 2004; Menza et al., 2007), and minor changes in water depth or quality can be devastating. However, there is no evidence for any

627 significant jump in sea-level from 10-8 ka on the GBR, leaving other perturbations to
628 be explored (Fig. 13).

629 A shelf-wide siliciclastic sediment flux has been well-discussed and constrained to
630 11-8 ka (Dunbar and Dickens, 2003; Page and Dickens, 2005). The authors
631 correlated a dark and siliciclastic-rich horizon across a 2700 km north-south transect
632 in sediment cores in the GBR, with the timing of sea-level crossing the shelf break
633 and the remobilisation of sediments. During this same period, (Webster et al., 2012)
634 presented new palynologic evidence from the northern GBR confirming a strong
635 mangrove signature within these horizons, indicating well-developed mangrove
636 communities on some parts of the adjacent shelf. Mass accumulation rates of both
637 siliciclastic and carbonate sediments peaked at about 10 ka across the shelf (Dunbar
638 and Dickens, 2003) (Fig. 13) with elevated, but significantly lower rates found in the
639 southern compared to the northern and central GBR (Page and Dickens, 2005).
640 From 8-6 ka, sedimentation had again reduced.

641 In spite of the evidence for a massive sediment flux, a clear indication of reduced
642 water quality is not apparent from the fossil communities on the shelf edge. Leading
643 up to the mesophotic coral hiatus, from 11-10 ka (and coincident with the start of the
644 sediment flux at 11 ka), communities were characterised by relatively diverse corals,
645 a high degree of encrustation (50-90%), and diverse and environmentally sensitive
646 epibionts, including mastophoroid coralline algae, consistent with clear, oligotrophic
647 waters of the GBR and other Indo-Pacific reefs (Gherardi and Bosence, 1999; Perry
648 and Smithers, 2006). However, *Celleporaria* sp., which thrive in turbid and
649 mesotrophic conditions (Hageman et al., 2003), was abundant locally at
650 Hydrographers Passage. While the fossil biota alone do not show a clear record of

651 increasing shelf edge sedimentation or turbidity, the close timing of the hiatus
652 observed at three of the four sites, and the observed period of maximum sediment
653 flux off the shelf in the central and northern GBR provides compelling evidence of a
654 causal relationship.

655 Similar to modern coral reefs, where multiple factors act in concert to reduce reef
656 resilience and induce demise (e.g., Anthony et al., 2011), the combined effects of
657 regional perturbations of sea-level rise, sediment flux, increased turbidity and
658 reduced light were most likely the factors responsible for the mesophotic reef demise
659 and subsequent hiatus. Most of the mesophotic corals were growing at the maximum
660 depth range of their modern counterparts immediately prior to the hiatus. At depths
661 greater than 60 m, coral abundance is sharply reduced in the modern mesophotic
662 community (Bridge et al., 2010; Bridge et al., 2011b), and the massive and tabular
663 corals are absent based on observations. Declines in coral abundance coupled with
664 diminished coral diversity, two effects of submergence beyond 60 m for these
665 communities, are key factors in reducing the resilience of a reef (see Nystrom et al.,
666 2008 for a review of ecological resilience). Additional extrinsic factors of sea-level
667 rise coupled with the sediment flux would have compressed coral habitats, possibly
668 reducing the depth of light attenuation by tens of metres. By 10 ka, wide swaths of
669 the outer shelf may have become temporarily degraded during the transgression due
670 to both the sediment flux and the increased depth. Reefs in palaeo-water depths as
671 shallow as 20-30 m on the outer shelf were affected (Webster et al., 2011), but those
672 initiating in shallow-water conditions on the inner and mid shelf (Hopley et al., 2007)
673 were apparently unaffected.

While the actual degree of turbidity during the sediment flux has not been quantified, mass accumulation rates are known to have risen by 4-5 times from 11-8 ka (Dunbar and Dickens, 2003; Page and Dickens, 2005). The rate of sea-level rise is also not well-constrained during this period for the GBR, though the transgression most likely continued until at least 7 ka (Lewis et al., 2012). Finally, whether 60 m depth is the 'tipping point' for mesophotic coral communities of the GBR, or the sea-level rise and sediment flux perturbations were extreme events cannot be decoupled from this dataset alone. Based only on the estimated effects of each of these three factors (sedimentation, sea-level and community changes), the mesophotic reefs would have been subjected to extreme environmental stress that exceeded their limits of tolerance.

Despite a chronologic data base of > 50 high resolution ages, the lack of corals from 10-8 ka is not indisputable evidence of a hiatus. Great care was taken to avoid any sampling bias, but material that was poorly preserved with extensive bioerosion was avoided due to contamination risk. Platy and encrusting corals were generally more heavily bioeroded and massive corals less so, meaning the final and deepest drowning community may not have been radiometrically dated in each case. Further work to reduce the possibility of bias, including additional radiometric dating with a focus on the platy and encrusting coralgal assemblage would be worthwhile. Estimates of the paleo-turbidity as sediment was transported across the shelf (Dunbar and Dickens, 2003), along with more precise reconstructions of the rate and amplitude of sea-level rise during the mesophotic hiatus, would also provide important environmental constraints.

4.4. Implications for modern mesophotic communities

Mesophotic communities are regarded as protected habitats, less-influenced by thermal stress and other disturbances (e.g., Bongaerts et al., 2010) than their shallow counterparts . However, studies show these deep communities are sensitive to not only some of the same perturbations as shallow-water reefs (e.g., Lesser and Slattery, 2011), but also to a unique suite of deep-water mortality events (e.g., Smith et al., 2010). The GBR fossil communities persisted through a lengthy period of environmental change and sea-level rise. During development from 13-10 ka, corals grew through deepening of about 30 m as well as the highest recorded volume of sediment flux across the shelf from 11-10 ka. To have tolerated such conditions might add weight to their interpretation as robust. However, ultimately these fossil mesophotic coral reef systems died, when they became less tolerant and more vulnerable, as paleowater depth increased to about 60 m while at the same time being subjected to high rates of sedimentation.

As unique ecosystems which are spatially variable and distinct from their shallow-water counterparts, establishing the local thresholds and limits of tolerance for modern mesophotic communities is crucial. Further work to identify mesophotic communities in the fossil record will provide essential long-term records of response, tolerance and thresholds to perturbations.

5. Conclusions

This study provides the first evidence that the submerged fossil corals reefs preserved along the shelf of the GBR also supported widespread fossil mesophotic coral communities at modern depths of 45-130 m. Based on their sedimentological, palaeo-ecological, and chronological characteristics, and compared with known sea-

level and their modern distribution, these communities developed episodically in mesophotic environments from 13 ka. These are the first fossil mesophotic coral communities to be comprehensively studied in the GBR from the last deglaciation. They offer valuable insight into tolerance and thresholds of these marginal communities during changing environmental conditions and we conclude that:

1. Based on the recovered modern and fossil assemblages, two distinct coralgal assemblages and one non-coral encruster assemblage are present on the shelf edge. The first assemblage is characterised by massive and tabular *Porites*, *Montipora* and faviids with mastophoroids and lithophylloids and secondary or minor melobesioid CCA components. The second assemblage is characterised by much thinner (< 2 cm), platy and encrusting coral morphologies, especially *Porites*, *Montipora* and agariciids, with associated melobesioids and *Sporolithon* and minor lithophylloids and mastophoroids. The third assemblage is dominated by foraminiferal and algal crusts, including melobesioids, *Peyssonnelia* and *Sporolithon* only.
2. Based on the modern distribution of the coralgal or non-coral encruster assemblage in each case, the massive/tabular community represents palaeo-water depths of < 60 m, the platy/encrusting coral community represents < 80-100 m, and the non-coral encruster community represents > 100 m.
3. Three distinct vertical patterns of overgrowth and biological succession are observed and represent stable photophilic (within the photic zone, < 100 m), photophilic-cryptic deepening (approaching the extreme edge of the photic zone at 100 m) and deeply submerged cryptic (>100 m) environmental settings.

4. Using >50 radiometric ages, two distinct generations of mesophotic coralgal community growth are identified, separated by a 2 ka hiatus. The first generation occurred from 13-10 ka at depths of 100-130 m and exhibits clear deepening signatures through time. This resulted in the drowning of the massive coralgal assemblage at 11-10 ka in three of the four study sites as palaeo-water depths increased to greater than 60 m. A hiatus in coral growth followed between 10-8 ka as the non-coral encrusters assemblages dominated. The second coralgal generation occurred from 8 ka to present at depths of 95 m to at least 45 m but does not exhibit deepening signatures.
5. Cessation of the first coral generation at 11-10 ka is coincident with modern reef initiation at ca. 30 m on the GBR as well as an increase in shelf-wide siliciclastic sediment flux. This suggests that coral communities are less resilient to perturbations when they are also persisting at their maximum depth tolerance, making them particularly vulnerable to other environmental changes.
6. Conditions were sufficiently restored by 8 ka, resulting in the re-population of the deep forereef slopes by similar mesophotic coralgal assemblages, with massive/tabular coral communities extending to 60 m, and platy/encrusting corals to 80-100 m.

Acknowledgements

We thank the captain and crew of the RV Southern Surveyor for their outstanding work on the cruise. This research was funded by the Australian Marine National Facility, the National Geographic Society, Australian Research Council (DP1094001) and the Natural Environment Research Council (NE/F523318/1). Radiocarbon ages

769 and XRD were funded by a postgraduate research grant awarded by the Australian
770 Institute of Nuclear Science and Engineering and facilities were provided by the
771 Australian Nuclear Science Technology Organisation. We acknowledge Paul Taylor
772 of the Natural History Museum, London for his contribution to the bryozoan
773 taxonomy. This paper is dedicated to the memory of Guy Cabioch, a friend and
774 fellow reef worker.

775

776 **References cited**

777 Abbey, E., Webster, J. M., Beaman, R. J., 2011a. Geomorphology of submerged reefs on
778 the shelf edge of the Great Barrier Reef: The influence of oscillating Pleistocene sea-
779 levels. Marine Geology 288, 61-78
780 Abbey, E., Webster, J. M., Braga, J. C., Sugihara, K., Wallace, C., Iryu, Y., Potts, D., Done,
781 T., Camoin, G., Seard, C., 2011b. Variation in deglacial coralgal assemblages and
782 their paleoenvironmental significance: IODP Expedition 310, "Tahiti Sea Level".
783 Global and Planetary Change 76 (1-2), 1-15
784 Adey, W. H., 1986. Coralline algae as indicators of sea-level, in: van de Plassche, O. (Ed.),
785 Sea-level research: A manual for the collection and evaluation of data. Geo Books,
786 Norwich, pp. 229-279.
787 Adey, W. H., Macintyre, I., Stuckenrath, R., 1977. Relict barrier reef system off St. Croix: Its
788 implications with respect to Late Cenozoic coral reef development in the western
789 Atlantic. Proceedings of the 3rd International Coral Reef Symposium 2, 15-21
790 Anthony, K. R. N., Connolly, S. R., 2004. Environmental limits to growth: physiological niche
791 boundaries of corals along turbidity–light gradients. Oecologia 141 (3), 373-384
792 Anthony, K. R. N., Maynard, J. A., Diaz-Pulido, G., Mumby, P. J., Marshall, P. A., Cao, L.,
793 Hoegh-Guldberg, O., 2011. Ocean acidification and warming will lower coral reef
794 resilience. Global Change Biology 17 (5), 1798-1808

795 Bak, R., Nieuwland, G., Meesters, E., 2005. Coral reef crisis in deep and shallow reefs:
796 30 years of constancy and change in reefs of Curacao and Bonaire. Coral Reefs 24
797 (3), 475-479
798 Bard, E., Hamelin, B., Arnold, M., Montaggioni, L., Cabioch, G., Faure, G., Rougerie, F.,
799 1996. Deglacial sea-level record from Tahiti corals and the timing of global meltwater
800 discharge. Nature 382 (6588), 241-244
801 Bard, E., Hamelin, B., Fairbanks, R. G., Zindler, A., 1990. Calibration of the ^{14}C timescale
802 over the past 30,000 years using mass spectrometric U-Th ages from Barbados
803 corals. Nature 345, 405-410
804 Beaman, R. J., Webster, J. M., Wüst, R. A. J., 2008. New evidence for drowned shelf edge
805 reefs in the Great Barrier Reef, Australia. Marine Geology 247 (1-2), 17-34
806 Blanchon, P., 2011. Back-Stepping, in: Hopley, D. (Ed.), Encyclopedia of Modern Coral
807 Reefs. Springer, New York, pp. 77-84.
808 Blanchon, P., Jones, B., Ford, D. C., 2002. Discovery of a submerged relic reef and
809 shoreline off Grand Cayman: further evidence for an early Holocene jump in sea
810 level. Sedimentary Geology 147 (3-4), 253-270
811 Bongaerts, P., Bridge, T. C. L., Kline, D., Muir, P., Wallace, C., Beaman, R., Hoegh-
812 Guldberg, O., 2011. Mesophotic coral ecosystems on the walls of Coral Sea atolls.
813 Coral Reefs, 1-1
814 Bongaerts, P., Ridgway, T., Sampayo, E., Hoegh-Guldberg, O., 2010. Assessing the 'deep
815 reef refugia' hypothesis: focus on Caribbean reefs. Coral Reefs 29 (2), 309-327
816 Bosence, D., 1983. Coralline algal reef frameworks. Journal of the Geological Society of
817 London 140, 365-376
818 Braga, J. C., Aguirre, J., 2004. Coralline algae indicate Pleistocene evolution from deep,
819 open platform to outer barrier reef environments in the northern Great Barrier Reef
820 margin. Coral Reefs 23, 547-558
821 Bridge, T., Done, T., Beaman, R., Friedman, A., Williams, S., Pizarro, O., Webster, J., 2010.
822 Topography, substratum and benthic macrofaunal relationships on a tropical

mesophotic shelf margin, central Great Barrier Reef, Australia. Coral Reefs 30 (1), 143-153

Bridge, T., Scott, A., Steinberg, D., 2012. Abundance and diversity of anemonefishes and their host sea anemones at two mesophotic sites on the Great Barrier Reef, Australia. Coral Reefs 31 (4), 1057-1062

Bridge, T. C. L., Done, T. J., Friedman, A., Beaman, R. J., Williams, S. B., Pizarro, O., Webster, J. M., 2011a. Variability in mesophotic coral reef communities along the Great Barrier Reef, Australia. Marine Ecology Progress Series 428, 63-75

Bridge, T. C. L., Fabricius, K. E., Bongaerts, P., Wallace, C. C., Muir, P., Done, T. J., Webster, J. M., 2011b. Diversity of Scleractinia and Octocorallia in the mesophotic zone of the Great Barrier Reef, Australia. Coral Reefs 31, 179-789

Brinkman, R., Wolanski, E., Deleersnijder, E., McAllister, F., Skirving, W., 2002. Oceanic inflow from the Coral Sea into the Great Barrier Reef. Estuarine, Coastal and Shelf Science 54 (4), 655-668

Burr, G. S., Galang, C., Taylor, F. W., Gallup, C., Edwards, R. L., Cutler, K., Quirk, B., 2004. Radiocarbon results from a 13-kyr BP coral from the Huon Peninsula, Papua New Guinea. Radiocarbon 46 (3), 1211-1224

Cabioch, G., Montaggioni, L., Frank, N., Seard, C., Salle, E., Payri, C., Pelletier, B., Paterne, M., 2008. Successive reef depositional events along the Marquesas foreslopes (French Polynesia) since 26 ka. Marine Geology 254 (1-2), 18-34

Cabioch, G., Montaggioni, L. F., Faure, G., Ribaud-Laurenti, A., 1999. Reef coralgal assemblages as recorders of paleobathymetry and sea level changes in the Indo-Pacific province. Quaternary Science Reviews 18 (14), 1681-1695

Camoin, G., Cabioch, G., Eisenhauer, A., Braga, J. C., Hamelin, B., Lericolais, G., 2006. Environmental significance of microbialites in reef environments during the last deglaciation. Sedimentary Geology 185 (3-4), 277-295

Camoin, G. F., Montaggioni, L. F., Braithwaite, C. J. R., 2004. Late glacial to post glacial sea levels in the Western Indian Ocean. Marine Geology 206, 119-146

851 Camoin, G. F., Seard, C., Deschamps, P., Webster, J. M., Abbey, E., Braga, J. C., Iryu, Y.,
852 Durand, N., Bard, E., Hamelin, B., 2012. Reef response to sea-level and
853 environmental changes during the last deglaciation: Integrated Ocean Drilling
854 Program Expedition 310, Tahiti Sea Level. Geology 40 (7), 643-646
855 Cheng, H., Edwards, R. L., Hoff, J., Gallup, C. D., Richards, D. A., Asmerom, Y., 2000. The
856 half lives of uranium-234 and thorium-230. Chemical Geology 169, 17-33
857 Davies, P. J., Braga, J. C., Lund, M., Webster, J. M., 2004. Holocene Deep Water Algal
858 Buildups on the Eastern Australian Shelf. Palaios 19 (6), 598-609
859 Deschamps, P., Durand, N., Bard, E., Hamelin, B., Camoin, G., Thomas, A. L., Henderson,
860 G. M., Okuno, J. i., Yokoyama, Y., 2012. Ice-sheet collapse and sea-level rise at the
861 Bolling warming 14,600[thinsp]years ago. Nature 483 (7391), 559-564
862 Druffel, E. R. M., Griffin, S., 1993. Large variations of surface ocean radiocarbon - evidence
863 of circulation changes in the southwestern Pacific. Journal of Geophysical Research-
864 Oceans 98 (C11), 20249-20259
865 Druffel, E. R. M., Griffin, S., 1999. Variability of surface ocean radiocarbon and stable
866 isotopes in the southwestern Pacific. Journal of Geophysical Research-Oceans 104
867 (C10), 23607-23613
868 Dullo, W. C., Camoin, G. F., Blomeier, D., Colonna, M., Eisenhauer, A., Faure, G.,
869 Casanova, J., Thomassin, B. A., 1998. Morphology and Sediments of the Fore-
870 Slopes of Mayotte, Comoro Islands: Direct Observations from a Submersible, Reefs
871 and Carbonate Platforms in the Pacific and Indian Oceans. Blackwell Publishing Ltd.
872 10.1002/9781444304879.ch11, pp. 217-236.
873 Dunbar, G. B., Dickens, G. R., 2003. Massive siliciclastic discharge to slopes of the Great
874 Barrier Reef Platform during sea-level transgression: constraints from sediment cores
875 between 15°S and 16°S latitude and possible explanations. Sedimentary Geology
876 162 (1-2), 141-158

877 Dunham, R. J., 1962. Classification of carbonate rocks according to depositional texture, in:
878 Ham, W. E. (Ed.), Classification of carbonate rocks. A symposium. American
879 Association of Petroleum Geologists, pp. 108-121.
880 Eakin, C. M., Morgan, J. A., Heron, S. F., Smith, T. B., Liu, G., Alvarez-Filip, L., Baca, B.,
881 Bartels, E., Bastidas, C., Bouchon, C., Brandt, M., Bruckner, A. W., Bunkley-
882 Williams, L., Cameron, A., Causey, B. D., Chiappone, M., Christensen, T. R. L.,
883 Crabbe, M. J. C., Day, O., de la Guardia, E., Diaz-Pulido, G., DiResta, D., Gil-
884 Agudelo, D. L., Gilliam, D. S., Ginsburg, R. N., Gore, S., Guzman, H. M., Hendee, J.
885 C., Hernandez-Delgado, E. A., Husain, E., Jeffrey, C. F. G., Jones, R. J., Jordan-
886 Dahlgren, E., Kaufman, L. S., Kline, D. I., Kramer, P. A., Lang, J. C., Lirman, D.,
887 Mallela, J., Manfrino, C., Marechal, J. P., Marks, K., Mihaly, J., Miller, W. J., Mueller,
888 E. M., Muller, E. M., Toro, C. A. O., Oxenford, H. A., Ponce-Taylor, D., Quinn, N.,
889 Ritchie, K. B., Rodriguez, S., Ramirez, A. R., Romano, S., Samhouri, J. F., Sanchez,
890 J. A., Schmahl, G. P., Shank, B. V., Skirving, W. J., Steiner, S. C. C., Villamizar, E.,
891 Walsh, S. M., Walter, C., Weil, E., Williams, E. H., Roberson, K. W., Yusuf, Y., 2010.
892 Caribbean Corals in Crisis: Record Thermal Stress, Bleaching, and Mortality in 2005.
893 Plos One 5 (11), e13969
894 Edwards, R. L., Chen, J. H., Wasserburg, G. J., 1986. ^{238}U-^{234}U-^{230}Th-^{232}Th systematics and
895 the precise measurement of time over the last 500,000 yaers. Earth and Planetary
896 Science Letters 81, 175-192
897 Faichney, I. D. E., Webster, J. M., Clague, D. A., Kelley, C., Appelgate, B., Moore, J. G.,
898 2009. The morphology and distribution of submerged reefs in the Maui-Nui Complex,
899 Hawaii: New insights into their evolution since the Early Pleistocene. Marine Geology
900 265 (3-4), 130-145
901 Fairbanks, R. G., 1989. A 17,000-year glacio-eustatic sea level record: influence of glacial
902 melting rates on the Younger Dryas event and deep-ocean circulation. Nature 342,
903 637-642

904 Fairbanks, R. G., 1990. The age and origin of the 'Younger Dryas climate event' in
905 Greenland ice cores. Paleoceanography 5, 937-948
906 Fairbanks, R. G., Mortlock, R. A., Chiu, T. C., Cao, L., Kaplan, A., Guilderson, T. P.,
907 Fairbanks, T. W., Bloom, A. L., Grootes, P. M., Nadeau, M. J., 2005. Radiocarbon
908 calibration curve spanning 0 to 50,000 years BP based on paired Th-230/U-234/U-
909 238 and C-14 dates on pristine corals. Quaternary Science Reviews 24 (16-17),
910 1781-1796
911 Fink, D., Hotchkis, M., Hua, Q., Jacobsen, G., Smith, A. M., Zoppi, U., Child, D., Mifsud, C.,
912 van der Gaast, H., Williams, A., Williams, M., 2004. The ANTARES AMS facility at
913 ANSTO. Nuclear Instruments and Methods in Physics Research Section B: Beam
914 Interactions with Materials and Atoms 223-224, 109-115
915 Flamand, B., Cabioch, G., Payri, C., Pelletier, B., 2008. Nature and biological composition of
916 the New Caledonian outer barrier reef slopes. Marine Geology 250, 157-179
917 Flügel, E., 2009. Microfacies of Carbonate Rocks: Analysis, Interpretation and Application,
918 2nd Edition. Springer, Berlin.
919 Fürstenau, J., Lindhorst, S., Betzler, C., Hübscher, C., 2010. Submerged reef terraces of the
920 Maldives (Indian Ocean). Geo-Marine Letters 30 (5), 511-515
921 Gherardi, D. F. M., Bosence, D. W. J., 1999. Modeling of the ecological succession of
922 encrusting organisms in Recent coralline-algal frameworks from Atol das Rocas,
923 Brazil. Palaios 14 (2), 145-158
924 Grigg, R. W., 2006. Depth limit for reef building corals in the Au'au Channel, SE Hawaii.
925 Coral Reefs 25 (1), 77-84
926 Grigg, R. W., Grossman, E. E., Earle, S. A., Gittings, S. R., Lott, D., McDonough, J., 2002.
927 Drowned reefs and antecedent karst topography, Au'au Channel, SE Hawaiian
928 Islands. Coral Reefs 21 (1), 73-82
929 Hageman, S. J., Lukasik, J., McGowran, B., Bone, Y., 2003. Paleoenvironmental
930 significance of Celleporaria (Bryozoa) from modern and tertiary cool-water
931 carbonates of southern Australia. Palaios 18 (6), 510-527

932 Hanebuth, T., Stattegger, K., Grootes, P. M., 2000. Rapid Flooding of the Sunda Shelf: A
933 Late-Glacial Sea-Level Record. Science 288 (5468), 1033-1035
934 Harris, P. T., Davies, P. J., 1989. Submerged reefs and terraces on the shelf edge of the
935 Great Barrier Reef, Australia - morphology, occurrence and implications for reef
936 evolution. Coral Reefs 8 (2), 87-98
937 Harris, P. T., Heap, A. D., Marshall, J. F., McCulloch, M. T., 2008. A new coral reef province
938 in the Gulf of Carpentaria, Australia: Colonisation, growth and submergence during
939 the early Holocene. Marine Geology 251 (1-2), 85-97
940 Harris, P. T., Heap, A. D., Wassenberg, T., Passlow, V., 2004. Submerged coral reefs in the
941 Gulf of Carpentaria, Australia. Marine Geology 207 (1-4), 185-191
942 Harris, P. T., Tsuji, Y., Marshall, J. F., Davies, P. J., Honda, N., Matsuda, H., 1996. Sand
943 and rhodolith-gravel entrainment on the mid- to outer-shelf under a western boundary
944 current: Fraser Island continental shelf, eastern Australia. Marine Geology 129 (3-4),
945 313-330
946 Hopley, D., Smithers, S. G., Parnell, K. E., 2007. The Geomorphology of the Great Barrier
947 Reef; development, diversity, and change. Cambridge University Press, Cambridge.
948 Hua, Q., Jacobsen, G., Zoppi, U., Lawson, E., Williams, A., McGann, M., 2001. Progress in
949 radiocarbon target preparation at the ANTARES AMS Centre. Radiocarbon 43 (2A),
950 275-282
951 Hughen, K. A., Baillie, M. G. L., Bard, E., Beck, J. W., Bertrand, C. J. H., Blackwell, P. G.,
952 Buck, C. E., Burr, G. S., Cutler, K. B., Damon, P. E., Edwards, R. L., Fairbanks, R.
953 G., Friedrich, M., Guilderson, T. P., Kromer, B., McCormac, G., Manning, S.,
954 Ramsey, C. B., Reimer, P. J., Reimer, R. W., Remmele, S., Southon, J. R., Stuiver,
955 M., Talamo, S., Taylor, F. W., van der Plicht, J., Weyhenmeyer, C. E., 2004.
956 MARINE04 marine radiocarbon age calibration, 0-26 cal kyr BP. Radiocarbon 46 (3),
957 1059-1086

958 Iryu, Y., Nakamori, T., Matsuda, S., Abe, O., 1995. Distribution of marine organisms and its
959 geological significance in the modern reef complex of the Ryukyu Islands.
960 Sedimentary Geology 99 (3-4), 243-258
961 Jarrett, B. D., Hine, A. C., Halley, R. B., Naar, D. F., Locker, S. D., Neumann, A. C., Twichell,
962 D., Hu, C., Donahue, B. T., Jaap, W. C., Palandro, D., Ciembronowicz, K., 2005.
963 Strange bedfellows - a deep-water hermatypic coral reef superimposed on a drowned
964 barrier island; southern Pulley Ridge, SW Florida platform margin. Marine Geology
965 214 (4), 295-307
966 Kahng, S., Garcia-Sais, J., Spalding, H., Brokovich, E., Wagner, D., Weil, E., Hinderstein, L.,
967 Toonen, R., 2010. Community ecology of mesophotic coral reef ecosystems. Coral
968 Reefs 29 (2), 255-275
969 King, B., McAllister, F., Wolanski, E., Done, T., Spagnol, S., 2001. River plume dynamics in
970 the central Great Barrier Reef, in: Wolanski, E. (Ed.), Oceanographic Processes of
971 Coral Reefs: Physical and biological links in the Great Barrier Reef. CRC Press,
972 Boca Raton, Floria, pp. 145-159.
973 Klovan, J. E., Embry, A. F., 1971. Upper Devonian stratigraphy, northeastern Banks Island,
974 N.W.T. Bulletin of Canadian Petroleum Geology 19 (4), 705-724
975 Lambeck, K., Chappell, J., 2001. Sea level change through the last glacial cycle. Science
976 292 (5517), 679-686
977 Lambeck, K., Yokoyama, Y., Johnston, P., Purcell, A., 2000. Global ice volumes at the Last
978 Glacial Maximum and early lateglacial. Earth and Planetary Science Letters 181 (4),
979 513-527
980 Larcombe, P., Woolfe, K. J., 1999. Terrigenous sediments as influences upon Holocene
981 nearshore coral reefs, central Great Barrier Reef, Australia. Australian Journal of
982 Earth Sciences 46 (1), 141-154
983 Lesser, M., Slattery, M., 2011. Phase shift to algal dominated communities at mesophotic
984 depths associated with lionfish (*Pterois volitans*) invasion on a Bahamian coral reef.
985 Biological Invasions 13 (8), 1855-1868

986 Lesser, M. P., Slattery, M., Leichter, J. J., 2009. Ecology of mesophotic coral reefs. Journal
987 of Experimental Marine Biology and Ecology 375, 1-8
988 Lewis, S. E., Sloss, C. R., Murray-Wallace, C. V., Woodroffe, C. D., Smithers, S. G., 2012.
989 Post-glacial sea-level changes around the Australian margin: a review. Quaternary
990 Science Reviews http://dx.doi.org/10.1016/j.quascirev.2012.09.006
991 Lighty, R. G., Macintyre, I., Stuckenrath, R., 1982. *Acropora palmata* reef framework: A
992 reliable indicator of sea level in the Western Atlantic for the past 10,000 years. Coral
993 Reefs 1, 125-130
994 Lund, M., Davies, P. J., Braga, J. C., 2000. Coralline algal nodules off Fraser Island, eastern
995 Australia. Facies 42 (1), 25-34
996 Macintyre, I. G., 1967. Submerged coral reefs, west coast of Barbados, West Indies.
997 Canadian Journal of Earth Sciences 4, 461-474
998 Macintyre, I. G., Rutzler, K., Norris, J. N., Smith, K. P., Cairns, S. D., Bucher, K. E., Steneck,
999 R. S., 1991. An early Holocene reef in the western Atlantic - submersible
1000 investigations of a deep relict reef off the west-coast of Barbados, W.I. Coral Reefs
1001 10 (3), 167-174
1002 Manning, M. P., Reid, R. C., 1977. CHO Systems in the Presence of an Iron Catalyst.
1003 Industrial & Engineering Chemistry Process Design and Development 16 (3), 358-
1004 361
1005 Marshall, J. F., Tsuji, Y., Matsuda, H., Davies, P. J., Iryu, Y., Honda, N., Satoh, Y., 1998.
1006 Quaternary and Tertiary subtropical carbonate platform development on the
1007 continental margin of southern Queensland, Australia, in: Camoin, G. F. and Davies,
1008 P. J. (Eds.), Reefs and Carbonate Platforms in the Pacific and Indian Oceans.
1009 Special Publications of the International Association of Sedimentologists, London, 25,
1010 pp. 163-195.
1011 Mason, A. J., Henderson, G. M., 2010. Correction of multi-collector-ICP-MS instrumental
1012 biases in high-precision uranium-thorium chronology. International Journal of Mass
1013 Spectrometry 295 (1-2), 26-35

1014 Menza, C., Kendall, M., Rogers, C., Miller, J., 2007. A deep reef in deep trouble. Continental
1015 Shelf Research 27 (17), 2224-2230
1016 Minnery, G. A., 1990. Crustose coralline algae from the Flower Garden Banks, northwestern
1017 Gulf of Mexico; controls on distribution and growth morphology. Journal of
1018 Sedimentary Research 60 (6), 992-1007
1019 Montaggioni, L. F., 2005. History of Indo-Pacific coral reef systems since the last glaciation:
1020 Development patterns and controlling factors. Earth-Science Reviews 71 (1-2), 1-75
1021 Nystrom, M., Graham, N. A. J., Lokrantz, J., Norstrom, A. V., 2008. Capturing the
1022 cornerstones of coral reef resilience: linking theory to practice. Coral Reefs 27 (4),
1023 795-809
1024 Page, M. C., Dickens, G. R., 2005. Sediment fluxes to Marion Plateau (southern Great
1025 Barrier Reef province) over the last 130 ky: New constraints on 'transgressive-
1026 shedding' off northeastern Australia. Marine Geology 219 (1), 27-45
1027 Peltier, W. R., 2002. On eustatic sea level history: Last Glacial Maximum to Holocene.
1028 Quaternary Science Reviews 21 (1-3), 377-396
1029 Peltier, W. R., Fairbanks, R. G., 2006. Global glacial ice volume and Last Glacial Maximum
1030 duration from an extended Barbados sea level record. Quaternary Science Reviews
1031 25, 3322-3337
1032 Perrin, C., 1992. Signification écologique des foraminifères acervulinidés et leur rôle dans la
1033 formation de faciès récifaux et organogènes depuis le Paléocène. Geobios 25 (6),
1034 725-751
1035 Perry, C. T., Smithers, S. G., 2006. Taphonomic signatures of turbid-zone reef development:
1036 Examples from Paluma Shoals and Lugger Shoal, inshore central Great Barrier Reef,
1037 Australia. Palaeogeography, Palaeoclimatology, Palaeoecology 242 (1-2), 1-20
1038 Pirazzoli, P. A., Montaggioni, L., 1988. The 7,000 year sea-level curve in French Polynesia:
1039 Geodynamic implications for mid-plate volcanic islands. Proceedings of the 6th
1040 International Coral Reef Symposium 3, 467-472

1041 Rao, V. P., Montaggioni, L., Vora, K. H., Almeida, F., Rao, K. M., Rajagopalan, G., 2003.
1042 Significance of relic carbonate deposits along the central and southwestern margin of
1043 India for late Quaternary environmental and sea level changes. Sedimentary Geology
1044 159 (1-2), 95-111
1045 Reed, J. K., 1985. Deepest distribution of Atlantic hermatypic corals discovered in the
1046 Bahamas. Proceedings of the 5th International Coral Reef Congress 6, 249-254
1047 Reimer, P. J., Baillie, M. G. L., Bard, E., Bayliss, A., Beck, J. W., Blackwell, P. G., Ramsey,
1048 C. B., Buck, C. E., Burr, G. S., Edwards, R. L., Friedrich, M., Grootes, P. M.,
1049 Guilderson, T. P., Hajdas, I., Heaton, T. J., Hogg, A. G., Hughen, K. A., Kaiser, K. F.,
1050 Kromer, B., McCormac, F. G., Manning, S. W., Reimer, R. W., Richards, D. A.,
1051 Southon, J. R., Talamo, S., Turney, C. S. M., van der Plicht, J., Weyhenmeye, C. E.,
1052 2009. INTCAL09 and MARINE09 radiocarbon age calibration curves, 0-50,000 years
1053 Cal BP. Radiocarbon 51 (4), 1111-1150
1054 Robinson, L. F., Belshaw, N. S., Henderson, G. M., 2004. U and Th concentrations and
1055 isotope ratios in modern carbonates and waters from the Bahamas. Geochim.
1056 Cosmochim. Acta 68, (8), 1777-1789
1057 Rozanski, K., Stichler, W., Gonfcantini, R., Scott, E., Beukens, R., Kromer, B., Plicht, J. d.,
1058 1992. The IAEA 14C Intercomparison Exercise 1990. Radiocarbon 34 (3), 506-519
1059 Salvat, B., Sibuet, M., Lambier, L., 1985. Benthic megafauna observed from the submersible
1060 Cyana on the fore-reef slope of Tahiti (French Polynesia) between 70 and 100 m.
1061 Proceedings of the 5th International Coral Reef Congress 1, 379-520
1062 Scott, E. M., 2006. Part 2: The Third International Radiocarbon Intercomparison (TIRI).
1063 Radiocarbon 45 (2), 293-398
1064 Siddiquie, H. N., 1975. Submerged Terraces in Laccadive-Islands, India. Marine Geology 18
1065 (5), M95-M101
1066 Smith, T., Blondeau, J., Nemeth, R., Pittman, S., Calnan, J., Kadison, E., Gass, J., 2010.
1067 Benthic structure and cryptic mortality in a Caribbean mesophotic coral reef bank

1068 system, the Hind Bank Marine Conservation District, U.S. Virgin Islands. Coral Reefs
1069 29 (2), 289-308
1070 Stuiver, M., Polach, H., 1977. Discussion: Reporting of ^{14}C data. Radiocarbon 19, 355-363
1071 Stuiver, M., Reimer, P. J., 1993. Extended C-14 Data-Base and Revised Calib 3.0 C-14 Age
1072 Calibration Program. Radiocarbon 35 (1), 215-230
1073 Toscano, M. A., Lundberg, J., 1999. Submerged Late Pleistocene reefs on the tectonically-
1074 stable SE Florida margin: high-precision geochronology, stratigraphy, resolution of
1075 Substage 5a sea-level elevation, and orbital forcing. Quaternary Science Reviews 18
1076 (6), 753-767
1077 Van Oppen, M. J. H., Bongaerts, P. I. M., Underwood, J. N., Peplow, L. M., Cooper, T. F.,
1078 2011. The role of deep reefs in shallow reef recovery: an assessment of vertical
1079 connectivity in a brooding coral from west and east Australia. Molecular Ecology 20
1080 (8), 1647-1660
1081 Veeh, H. H., Veevers, J. J., 1970. Sea-level at -175 m off the Great Barrier Reef 13,6000 to
1082 17,000 years ago. Nature 226, 536-537
1083 Veron, J. E. N., 1986. Corals of Australia and the Indo-Pacific. Angus & Robertson, North
1084 Ryde, N.S.W.
1085 Veron, J. E. N., 2000. Corals of the World. Australian Insitute of Marine Science, Townsville.
1086 Veron, J. E. N., Pichon, M., 1979. Families Agariciidae, Siderastreidae, Fungiidae,
1087 Oculinidae, Merulinidae, Mussidae, Pectiniidae, Caryophylliidae, and
1088 Dendrophylliidae, Scleractinia of Eastern Australia Part 3. Australian Institute of
1089 Marine Science, Townsville, Australia, Vol. 4, pp. 1-422.
1090 Veron, J. E. N., Pichon, M., 1982. Family Poritidae, Scleractinia of Eastern Australia Part 4.
1091 Australian Institute of Marine Science, Townsville, Australia, Vol. 5, pp. 1-159.
1092 Veron, J. E. N., Pichon, M., Wijsman-Best, M., 1977. Families Faviidae and Trachyphylliidae,
1093 Scleractinia of Eastern Australia Part 2. Australian Institute of Marine Science,
1094 Townsville, Australia, Vol. 3, pp. 1-233.

1095 Veron, J. E. N., Wallace, C. C., 1984. Family Acroporidae, Scleractinia of Eastern Australia
1096 Part 5. Australian Institute of Marine Science, Townsville, Australia, Vol. 6, pp. 1-
1097 483.
1098 Vogel, J. S., Southon, J. R., Nelson, D. E., Brown, T. A., 1984. Performance of catalytically
1099 condensed carbon for use in accelerator mass spectrometry. Nuclear Instruments &
1100 Methods in Physics Research B5 5, 289-293
1101 Vora, K. H., Wagle, B. G., Veerayya, M., Almeida, F., Karisiddaiah, S. M., 1996. 1300 km
1102 long late Pleistocene-Holocene shelf edge barrier reef system along the western
1103 continental shelf of India: Occurrence and significance. Marine Geology 134 (1-2),
1104 145-162
1105 Wagle, B. G., Vora, K. H., Karisiddaiah, S. M., Veerayya, M., Almeida, F., 1994. Holocene
1106 submarine terraces on the western continental-shelf of India - implications for sea-
1107 level changes. Marine Geology 117 (1-4), 207-225
1108 Webster, J. M., Beaman, R. J., Puga-Bernabéu, Á., Ludman, D., Renema, W., Wust, R. A.
1109 J., George, N. P. J., Reimer, P. J., Jacobsen, G. E., Moss, P., 2012. Late Pleistocene
1110 history of turbidite sedimentation in a submarine canyon off the northern Great
1111 Barrier Reef, Australia. Palaeogeography, Palaeoclimatology, Palaeoecology 331-
1112 332, 75-89
1113 Webster, J. M., Clague, D. A., Riker-Coleman, K., Gallup, C., Braga, J. C., Potts, D., Moore,
1114 J. G., Winterer, E. L., Paull, C. K., 2004. Drowning of the -150 m reef off Hawaii: A
1115 casualty of global meltwater pulse 1A? Geology 32 (3), 249-252
1116 Webster, J. M., Davies, P. J., Beaman, R. J., Williams, S., Byrne, M., 2008. Evolution of
1117 drowned shelf edge reefs in the GBR; implications for understanding abrupt climate
1118 change, coral reef response and modern deep water benthic habitats—RV Southern
1119 Survey - voyage summary. Marine National Facility, Hobart, Tasmania.
1120 Webster, J. M., Yokoyama, Y., Cotterill, C., and the Expedition 310 Scientists, 2011.
1121 Proceedings of the IODP, 325. Integrated Ocean Drilling Program Management
1122 International, Inc., Tokyo.

Woodroffe, C. D., Brooke, B. P., Linklater, M., Kennedy, D. M., Jones, B. G., Buchanan, C., Mleczko, R., Hua, Q. A., Zhao, J. X., 2010. Response of coral reefs to climate change: Expansion and demise of the southernmost Pacific coral reef. Geophysical Research Letters 37, L152602

Wright, V. P., 1992. A revised classification of limestones. Sedimentary Geology 76 (3-4), 177-185

Yokoyama, Y., Esat, T. M., Lambeck, K., Fifield, L. K., 2000. Last ice age millennial scale climate changes recorded in Huon Peninsula corals. Radiocarbon 42 (3), 383-401

Yokoyama, Y., Purcell, A., Lambeck, K., Johnston, P., 2001. Shore-line reconstruction around Australia during the Last Glacial Maximum and Late Glacial Stage. Quaternary International 83-5, 9-18

Yokoyama, Y., Purcell, A., Marshall, J. F., Lambeck, K., 2006. Sea-level during the early deglaciation period in the Great Barrier Reef, Australia. Global and Planetary Change 53, 147-153

Figure captions

Fig. 1. Four sites along the eastern margin of the Great Barrier Reef (GBR) were mapped using multibeam sonar (Abbey et al., 2011a) and dredged between depths of ca. 45-170 m. Regions include A) Ribbon Reef, B) Noggin Pass, C) Viper Reef and D) Hydrographers Passage. Details of boxed regions around dredges can be found in Fig. 2.

Fig. 2. Bathymetry (5x vertical exaggeration) overlain by dredging tracks (black lines). “Dr2”=Dredge 2. Dredge coordinates, distances and depth ranges can be found in Table 1. Distance of dredge tracks are labelled here in black text for scale, and contours are labelled in white. For a detailed description of the regional geomorphology see Abbey et al. (2011a).

Fig. 3. Modern coral and coralline algae distribution determined from dredges. Corals and algae were either living when collected or identified as modern through AMS and U-Th dating. Depth ranges are only determined from those corals and coralline algae which were collected in situ. Grey bands indicate depth ranges which were dredged. Major coral and algae groups are labelled.

Fig. 4. Distribution of internal biota and coral morphology by geomorphologic feature. External non-coral encrusting biota are addressed in Fig. 6.

Fig. 5. A) D4-1 *Lithophyllum insipidum* (modern); B) D4-3 *Lithothamnion prolifer* with conceptacles (modern); C) D8-56 *Lithoporella sp.* (modern?); D) D22-4 *Mesophyllum funafutiense* (fossil).

Fig. 6. A) Graphical representation of the five abundance categories for non-coral encrusting biota. B) Non-coral encruster distribution by geomorphological feature and relative abundance.

Fig. 7 Representative examples of an A) indurated boundstone facies comprising laminated layers of CCA (white layers) and hemipelagic mud (dark layers); B) floatstone facies comprising disarticulated *Halimeda* plates in a fine-grained matrix; C) macroid facies comprising a nucleus with successive overgrowths of thin CCA (e) and thick acervulinids (a); D) coralgal boundstone facies comprising successive overgrowths of corals (c) and CCA (e).

Fig. 8. Facies distribution and relative abundance by geomorphological feature.

Fig. 9. Models of vertical biologic succession. A) Stable photophilic succession characterised by the alternation of corals and CCA. B) Photophilic-cryptic succession, characterised by photophilic biota, usually a coral with CCA, overgrown by cryptic biota, usually acervulinids or bryozoan. C) Stable cryptic succession characterised by alternating layers of acervulinids, CCA and/or bryozoan and the exclusion of photophilic corals.

Fig. 10. Radiometric dating results symbolised by (A) the taxonomy and site of the dated material and (B) the bio-litho facies (see Table 6 for facies descriptions and Table 3 for details of radiometric dating). Paired AMS-U-Th ages are indicated with an arrow and all others are AMS only.

Fig. 11. Age vs. depth of coralgal assemblages (if identified) or biota (if assemblage unidentified). Coloured vertical bars represent palaeo-water depth range of the massive/tabular (red) and encrusting/platy (yellow) coralgal assemblages and

1185 dashed lines incorporate dredging depth error. Black vertical error is derived from
1186 dredging range and horizontal error is AMS 2σ. Arrows identify reworked limestones.
1187 Sea-level data by Lambeck and Chappell, 2002 is for indicative purposes only and
1188 may not be directly applicable to the GBR (see Yokoyama et al., 2006 for a
1189 discussion on deglacial sea-level calculations on the GBR).

1190 Fig. 12. Schematic of the vertical succession of biota on a shelf edge profile across
1191 submerged reefs and terraces. Successions are based on radiometric dating.
1192 Drowned shallow-water reef generations (RG; sensu Montaggioni, 2005) form the
1193 foundation for later mesophotic communities. The first mesophotic generation was
1194 formed by massive corals at depths of 85-130 m. From 13.0-10.2 ka, massive corals
1195 were succeeded by encrusting and platy growth forms and ultimately by encrusting
1196 coralline algae and bryozoans. The second mesophotic generation was formed by
1197 encrusting and platy corals from 80-100 m and by massive corals from 45-60 m. This
1198 coral growth did not recommence until 7.8 ka, leaving a period of ca. 2 ky as a
1199 possible hiatus of mesophotic growth, coinciding with modern reef initiation on the
1200 GBR.

1201 Fig. 13. Summary of age relationships between fossil mesophotic and shallow water
1202 reefs in the GBR. The radiocarbon ages of corals summarised in Larcombe et al.
1203 (1999) have been recalibrated using the same method as described in the text.
1204 Corals collected from inter-reef areas have been excluded. Hopley et al. (2007) ages
1205 have also been recalibrated here. Three IODP Exp. 325 ages were omitted due to
1206 clear evidence of post-mortem transportation. In a comparison with known meltwater
1207 pulses and environmental perturbations, the hiatus of the first generation of
1208 mesophotic growth (indicated) appears to be coincident in timing with the siliciclastic

1209 flux (yellow bar) (described in Dunbar and Dickens, 2003; Page and Dickens, 2005).
1210 Coral growth recommenced about 1 ky after the start of the flux on the modern reefs,
1211 and about 2 ky in the mesophotic communities.

1212 **Table captions**

1213 Table 1. Location, bathymetric range and morphologic setting of dredges. See also
1214 Figs. 1 and 2 for dredge locations.

1215 Table 2. U-Series isotope data: Activity ratios are presented according to the decay
1216 constants of Cheng et al. (2000, their Table 3).

1217 Table 3. Taxonomy of all identified biota, modern (superscript 'M') and fossil
1218 (superscript 'F').

1219 Table 4. Coral taxon distribution by dredge. The number of asterisks (*) indicates
1220 relative abundance.

1221 Table 5. Coralgal and non-coral encruster assemblage characteristics and modern
1222 distribution.

1223 Table 6. Bio-litho facies descriptions.

1224 Table 7. Spatial distribution of facies and biota by morphologic feature at each site.
1225 Facies are described in order of abundance and abbreviations are as follows:
1226 BD=boundstone, IC=isolated colony, RH=rhodolith, MC=macroid, IBD=indurated
1227 boundstone, CN=crystalline, GR=grainstone, FL=floatstone, RD=rudstones,
1228 SH=shellstone, CM=calcimudstone. Boundstone qualifiers include c=coral,
1229 f=foraminifera and a=algal. See Table 6 for facies descriptions. Modern corals and
1230 CCA are those that were collected with living tissue or confirmed modern through ^{AMS}
1231 and U-Th dating. Recent corals still retain their surface ornamentation. See text for
1232 classification as in situ.

Table 8. Radiocarbon dating results. Biota are described in order of vertical succession (i.e. base to top, or inner to outer). T=transported or reworked, I.S.=in situ. Calibrated median ages are reported in years before 1950 CE. An age of 0 (zero) indicates the radiocarbon activity is too high (young) to be calibrated using the MARINE09 calibration curve. Calcite quantification was only performed on corals. Pooled means are calculated for corals that underwent replicate radiocarbon dating (OZ lab codes only).

Table 9. U-Series ages: [a]U-Th ages calculated assuming a closed system and no correction for initial ^{230}Th, all ages are presented in thousands of calendar years before AD1950 (i.e. -0.011 ka = 1961 CE). [b](^{234}U/^{238}U) at the time at which the coral grew was calculated using the uncorrected age. Corrected ages are based on a contaminant phase bearing Th with a (^{230}Th/^{232}Th) estimated from the geochemical database GEOROC (http://georoc.mpch-mainz.gwdg.de).

Graphical Abstract (for review)

Graphical Abstract

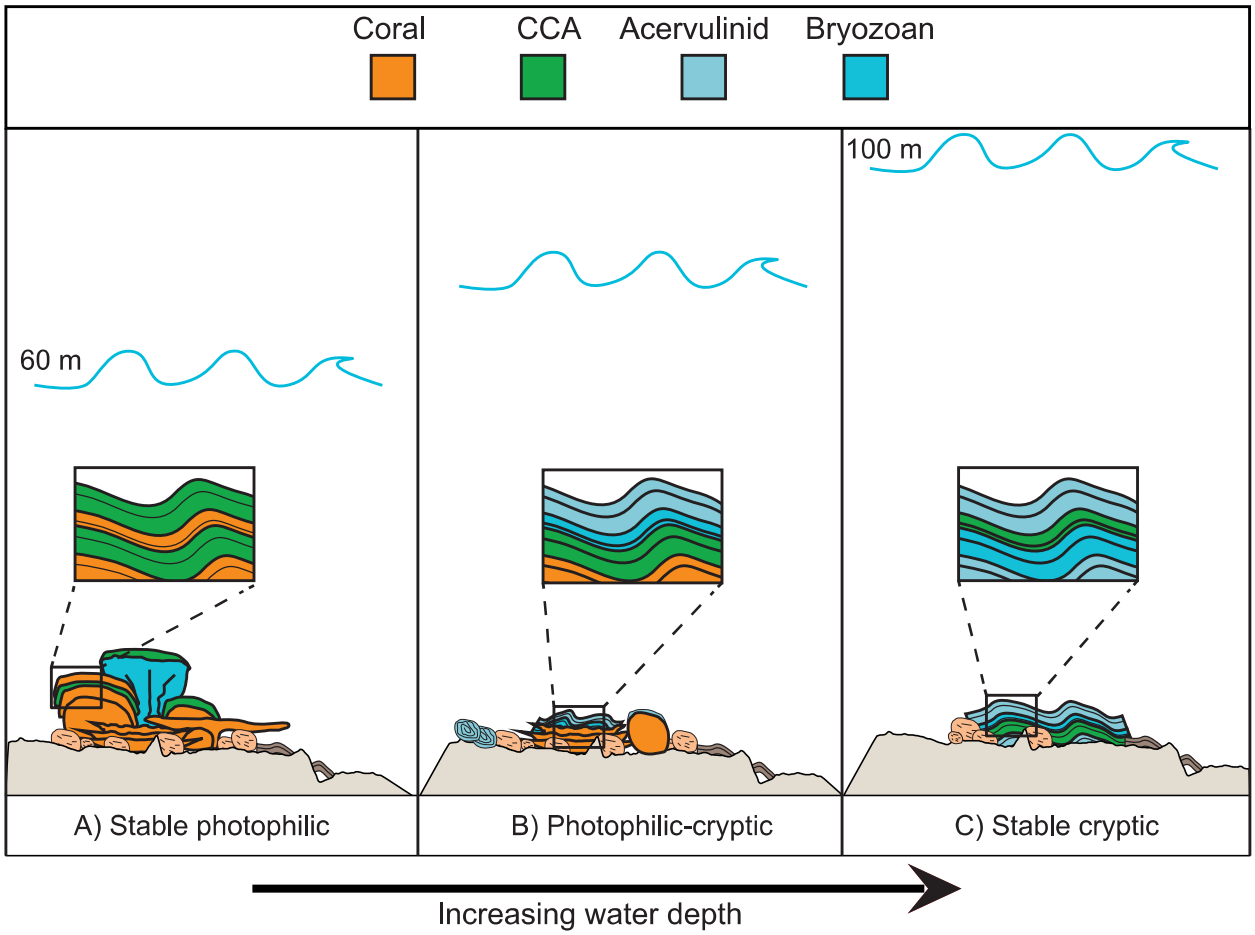

Highlights (to be submitted in a separate file, 85 characters each including spaces)

1. We describe 3 deglacial mesophotic assemblages and interpret their environments.
2. Extensive radiometric dating constrains the timing of their development.
3. We identify a period of perturbation where mesophotic coral growth is interrupted.
4. The hiatus coincides with massive sediment flux attributed to sea level rise.

Figure

Figure 1. Multibeam bathymetry and dredge locations

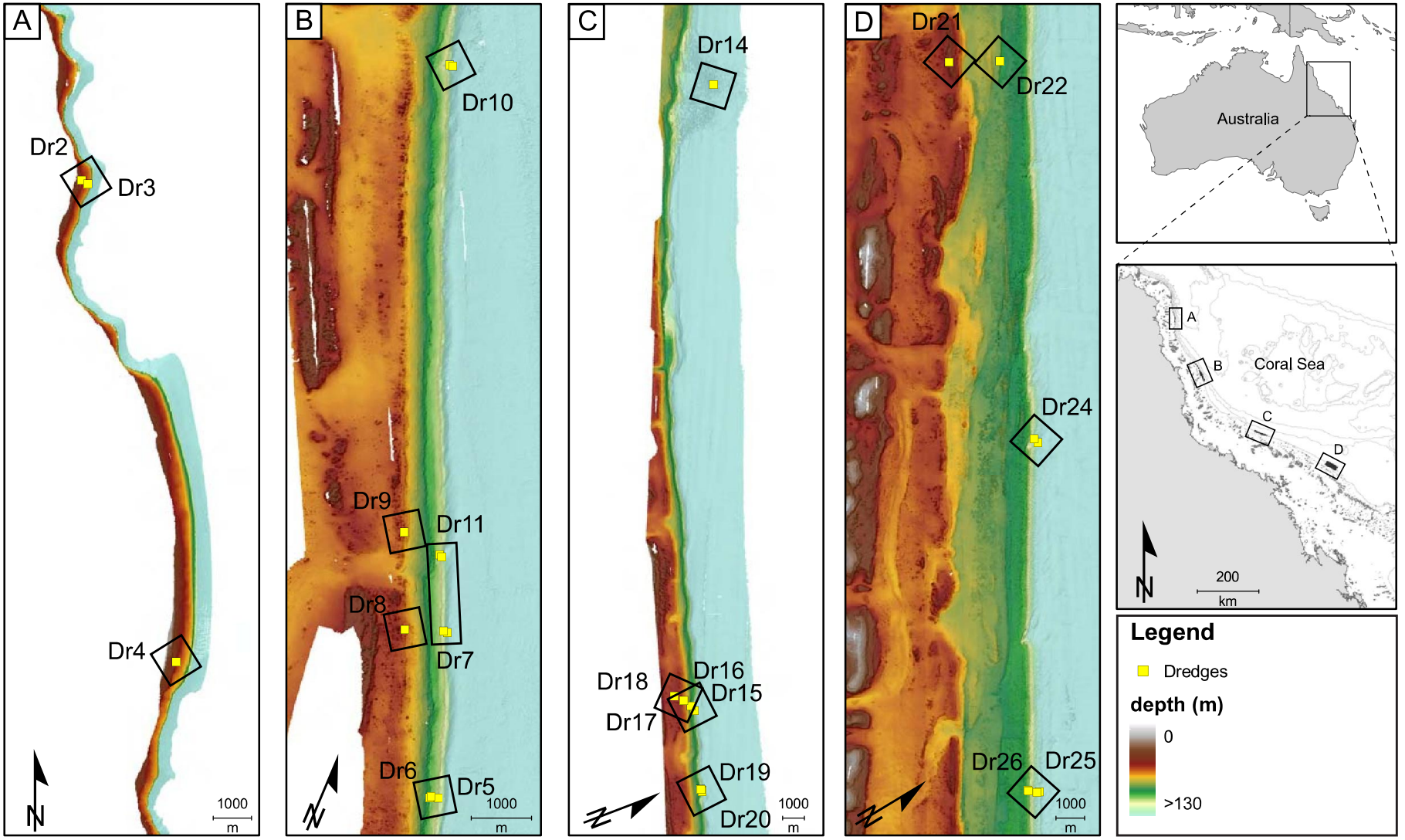

Figure 2. Dredge location and context

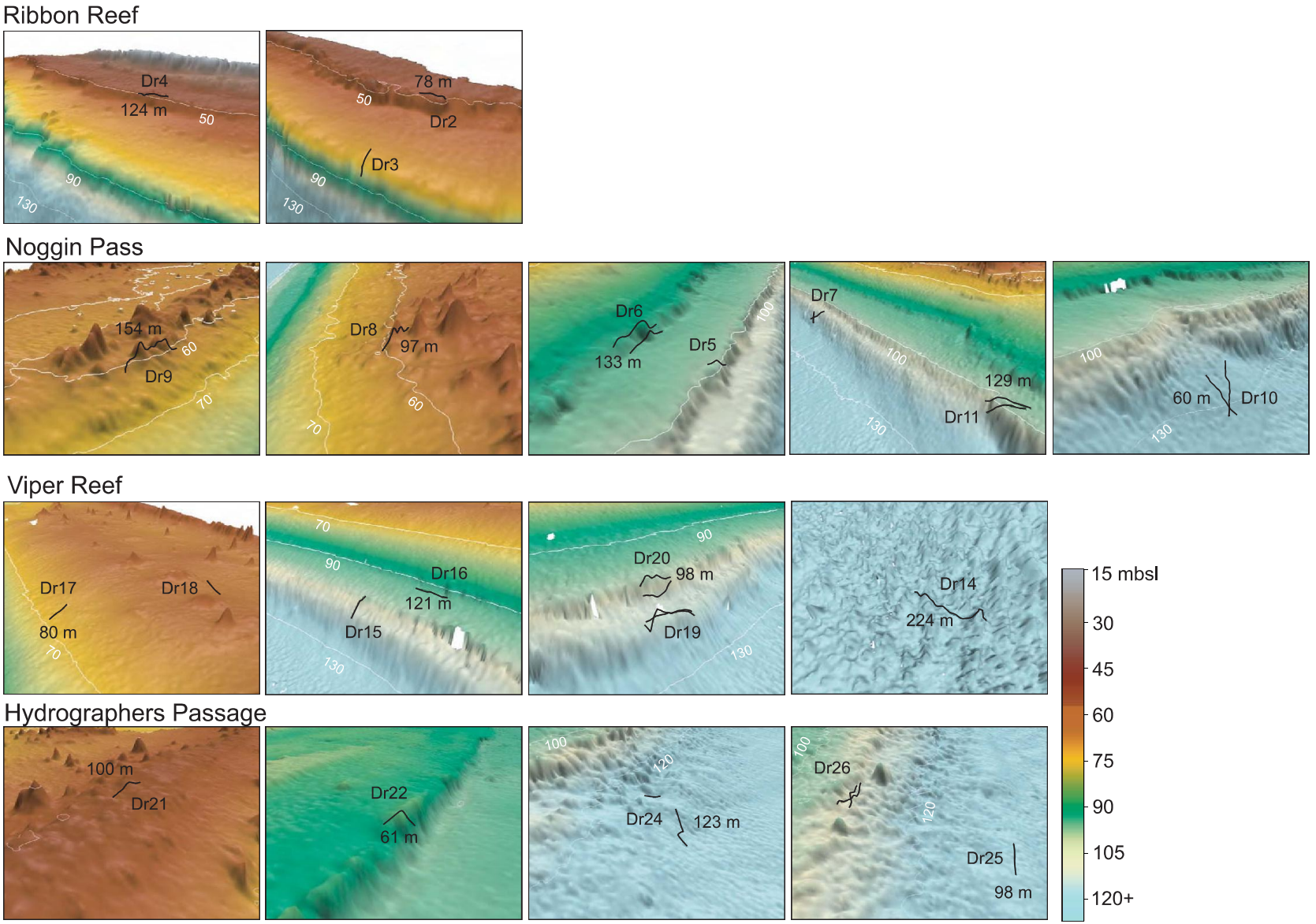

Figure

Figure 3. Coral and algae depth distribution

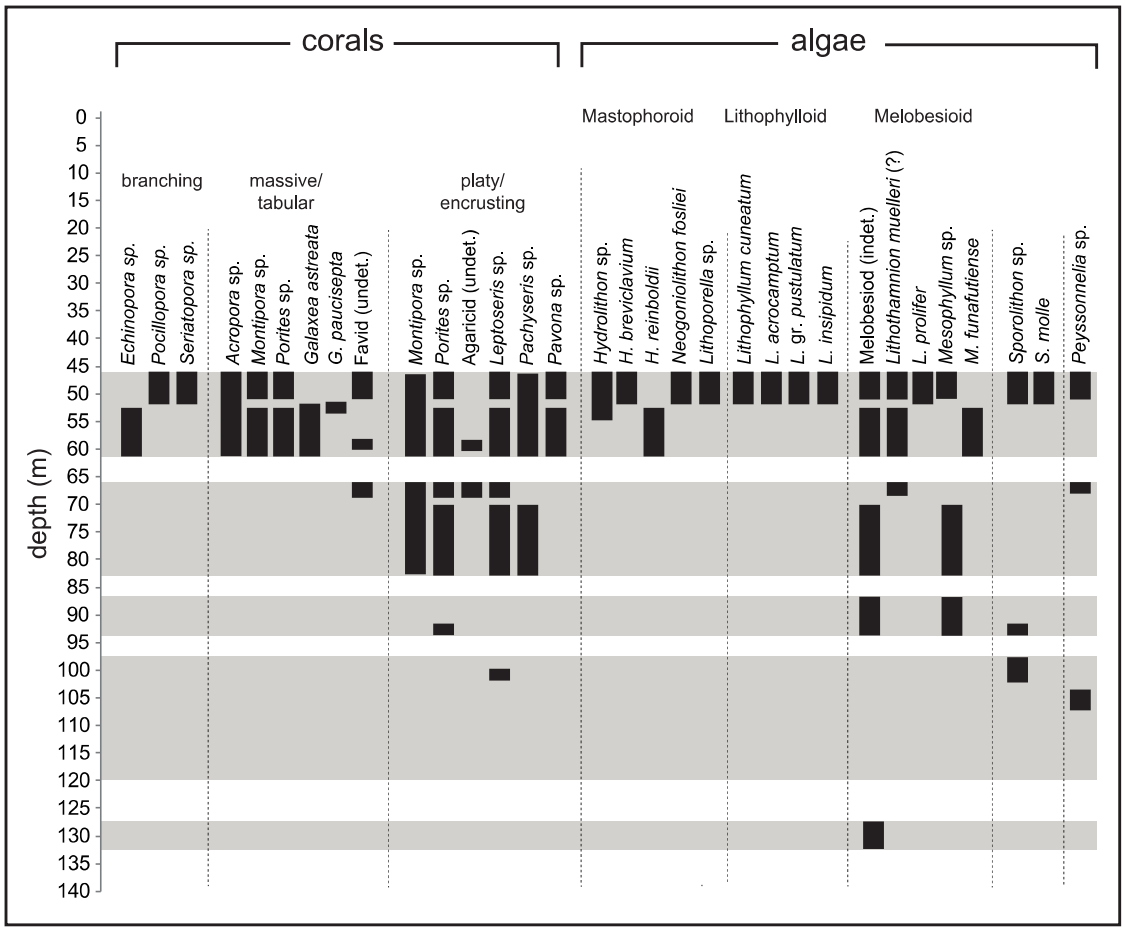

Figure 4. Biota distribution

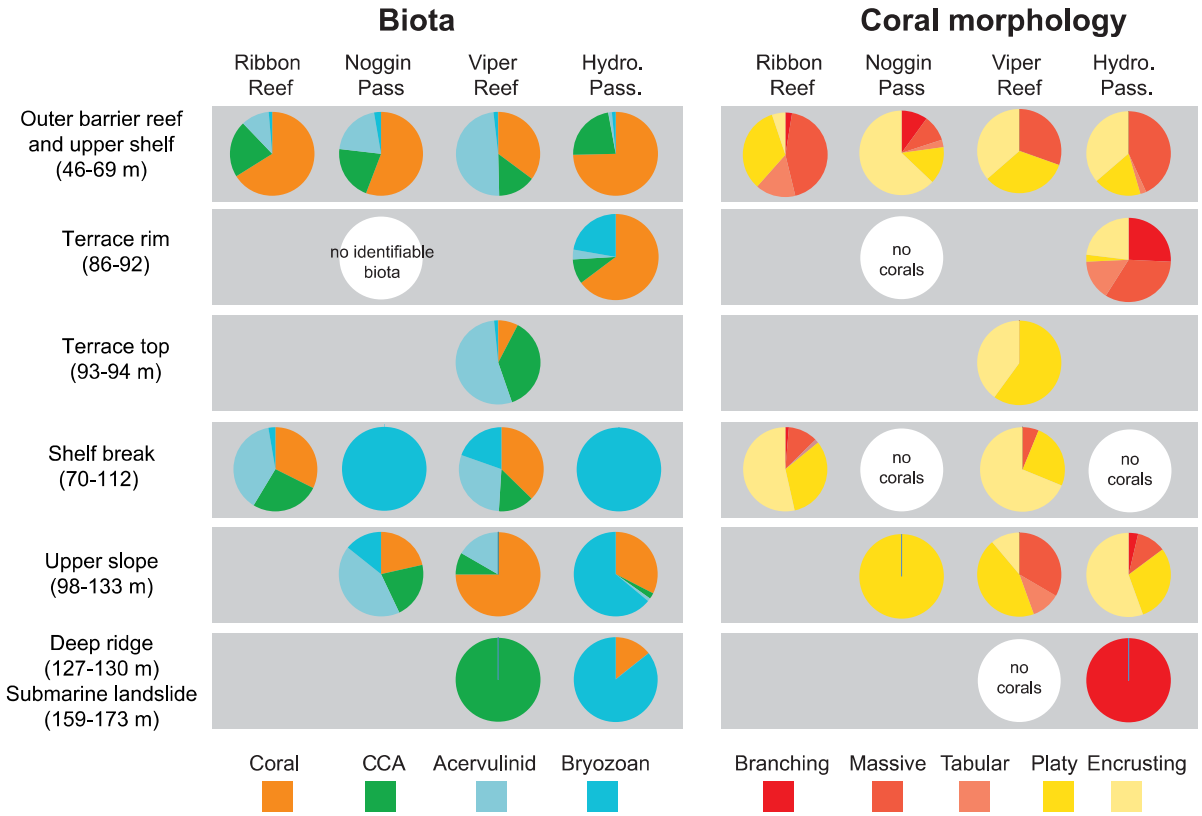

Figure

Figure 5. Coralline algal and foraminferal assemblages

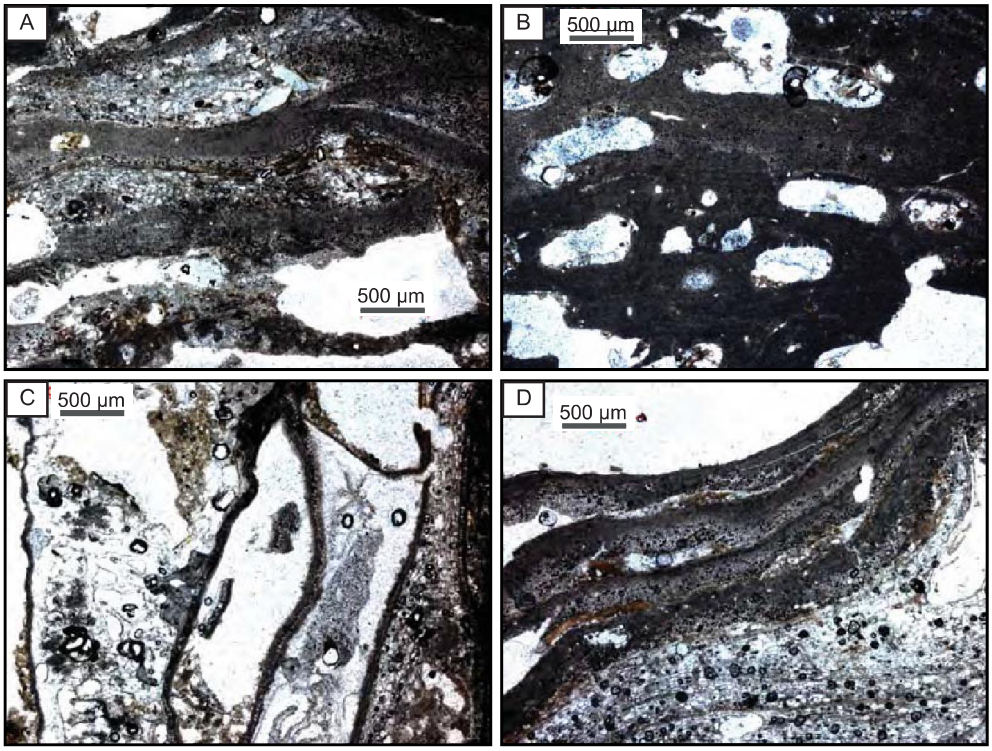

Figure

Figure 6. Distrubution of encrusting biota

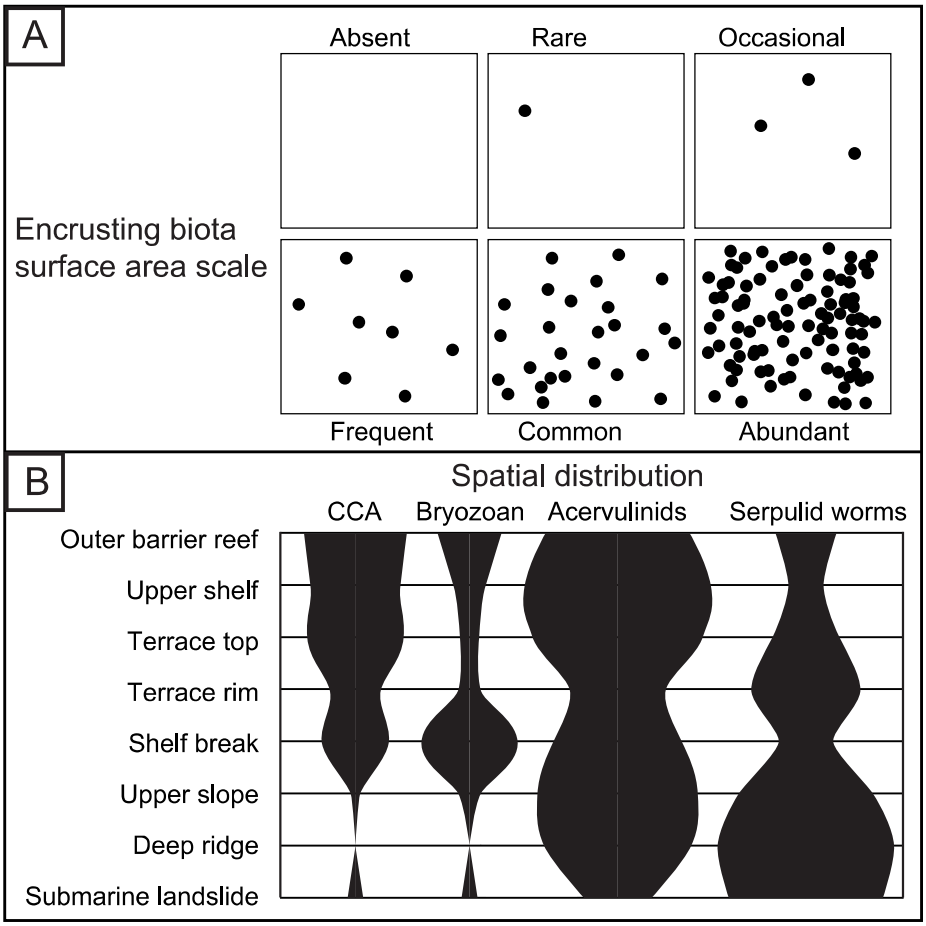

Figure

Figure 7. Representative sedimentary facies

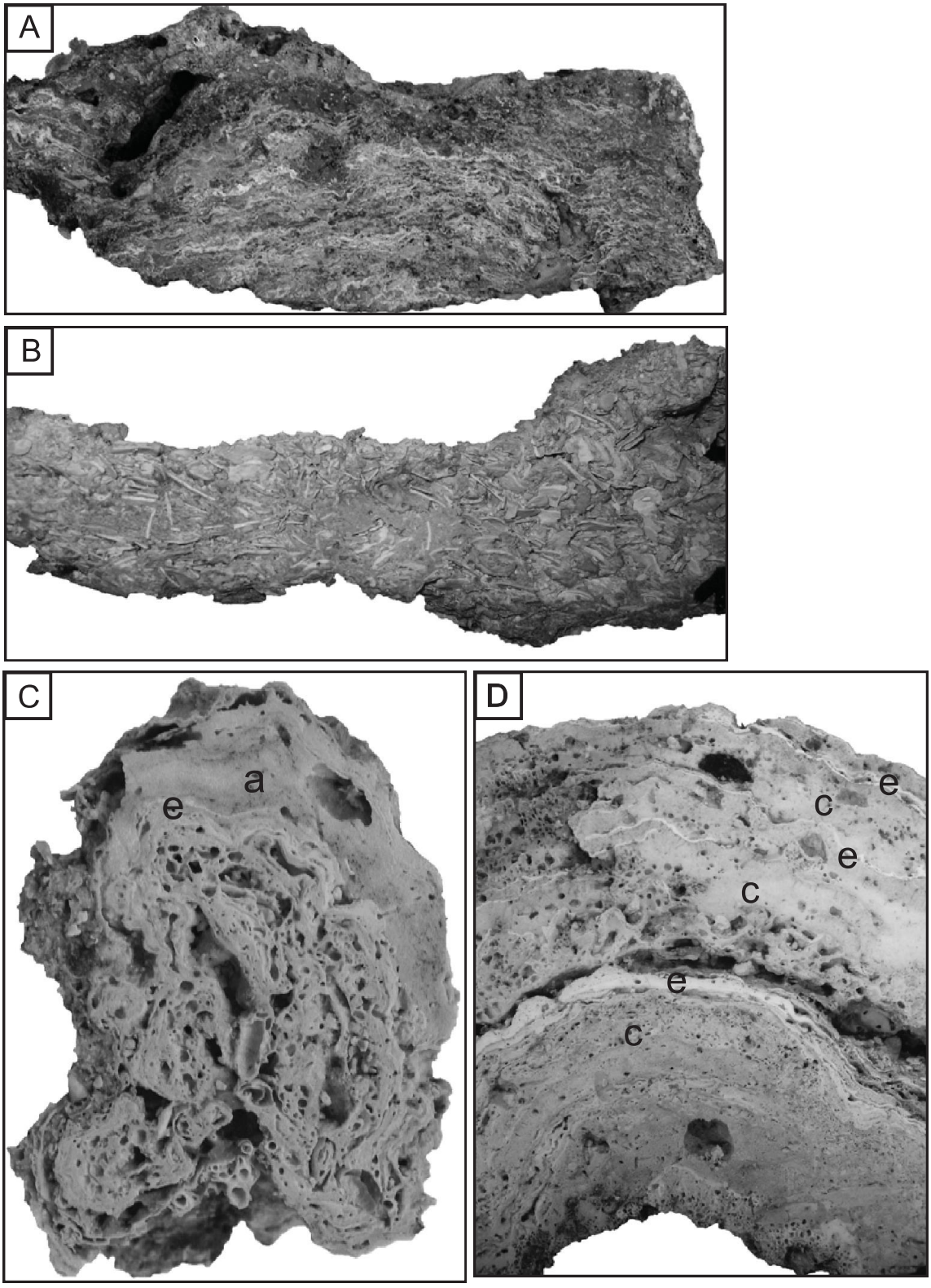

Figure

Figure 8. Distrubution of sedimentary facies

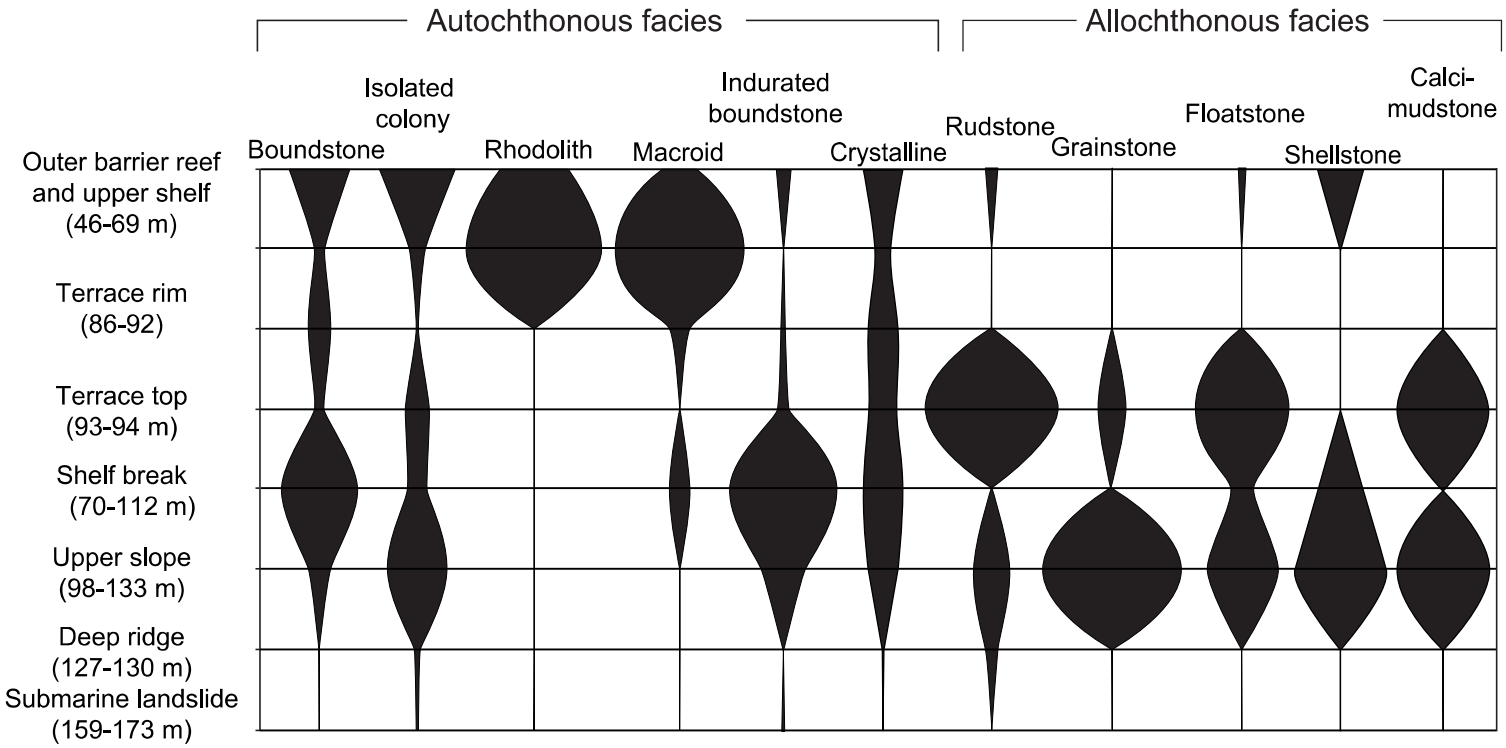

Figure 9. Models of ecological succession

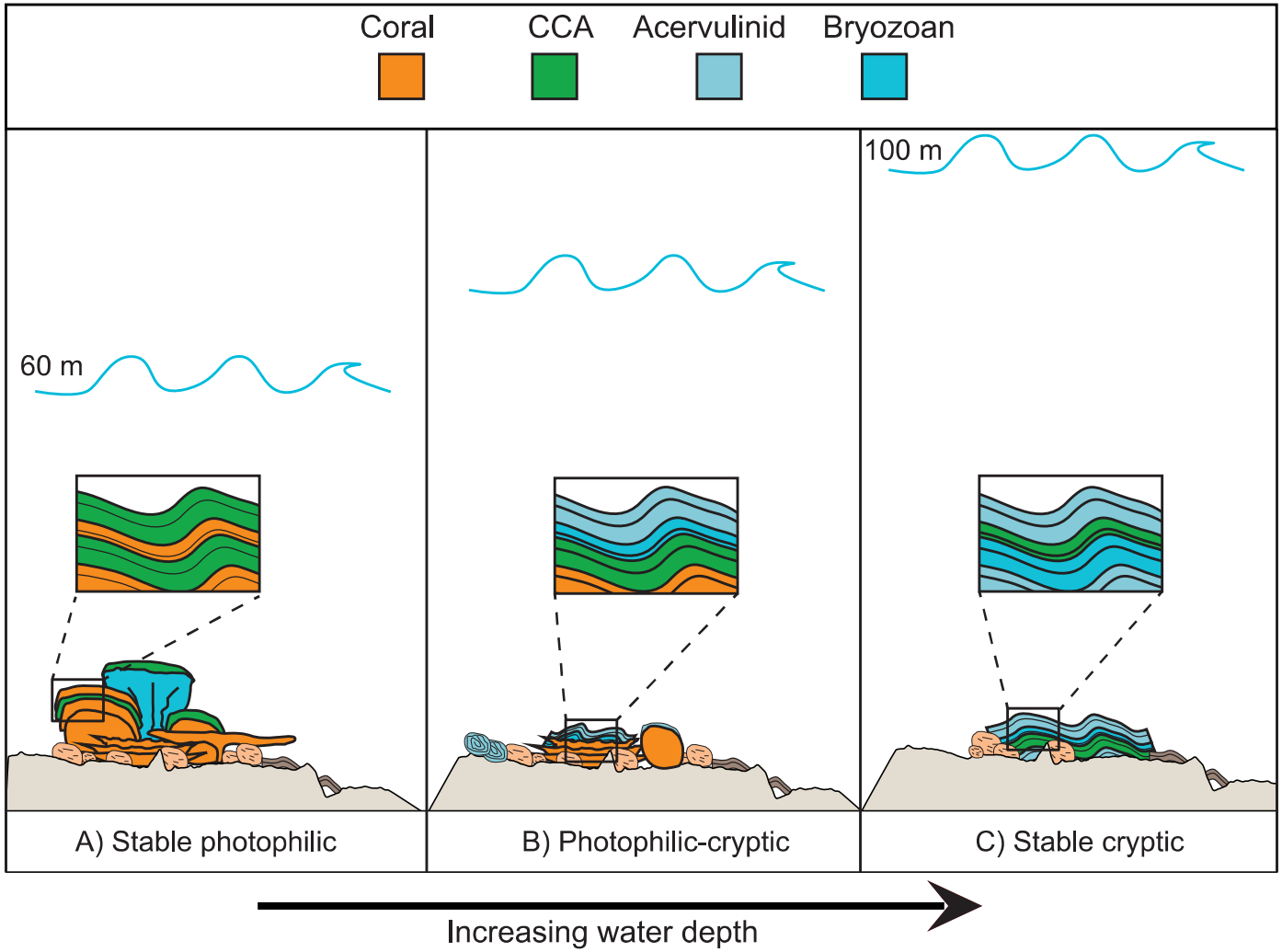

Figure

Figure 10. Radiometric data

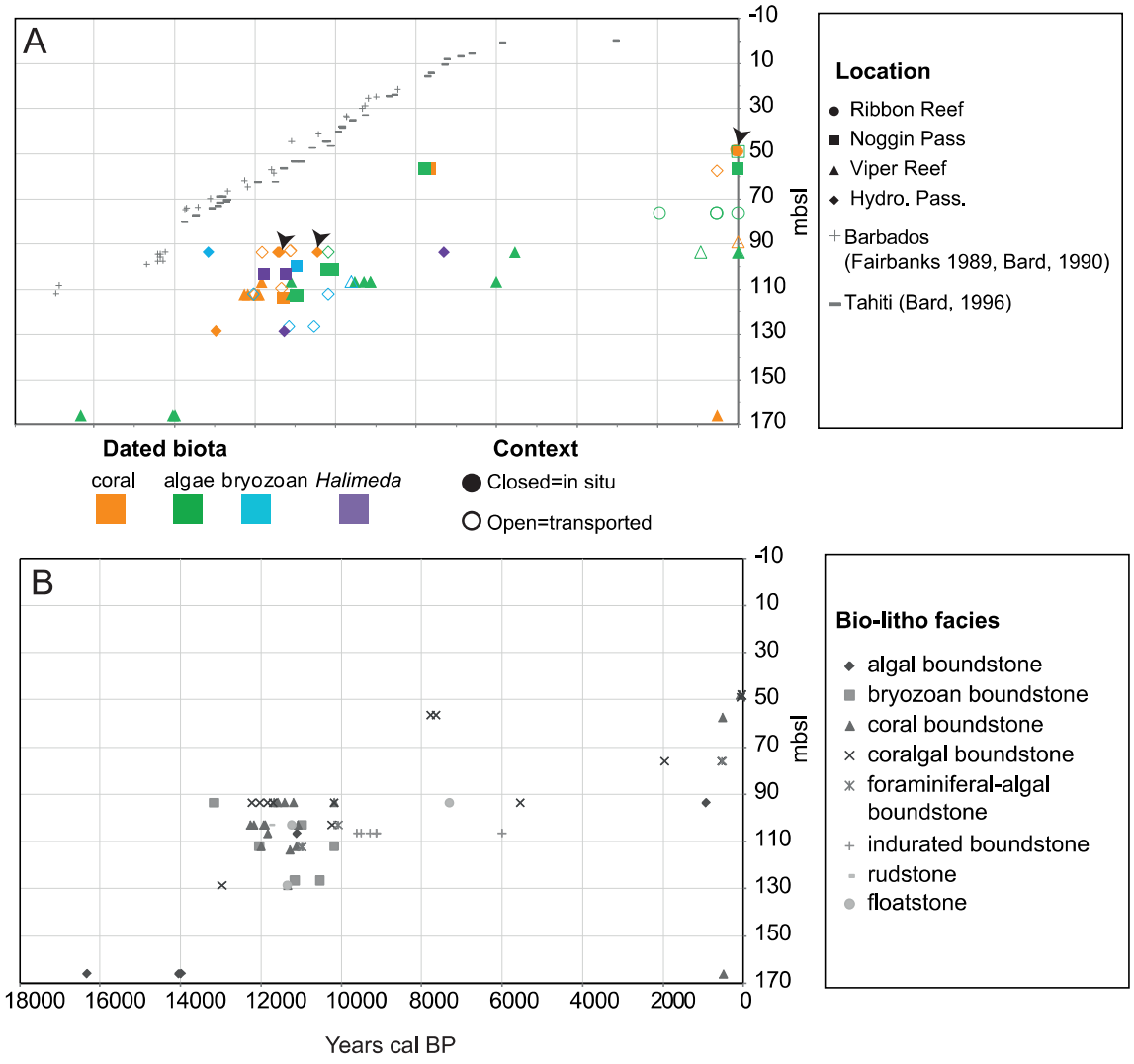

Figure

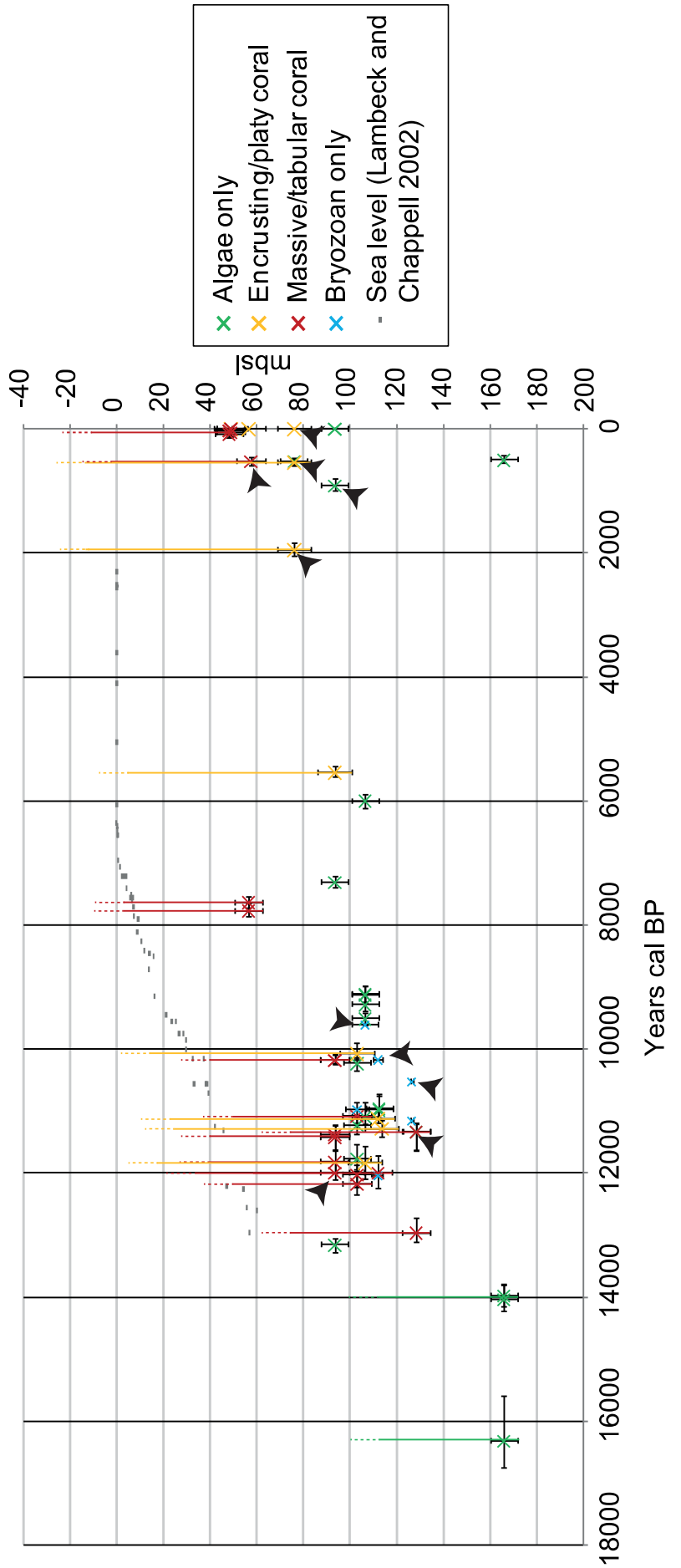

Figure 11. Age vs depth of coralgal assemblages

Figure 12. Schematic of the succession of biota on the shelf edge.

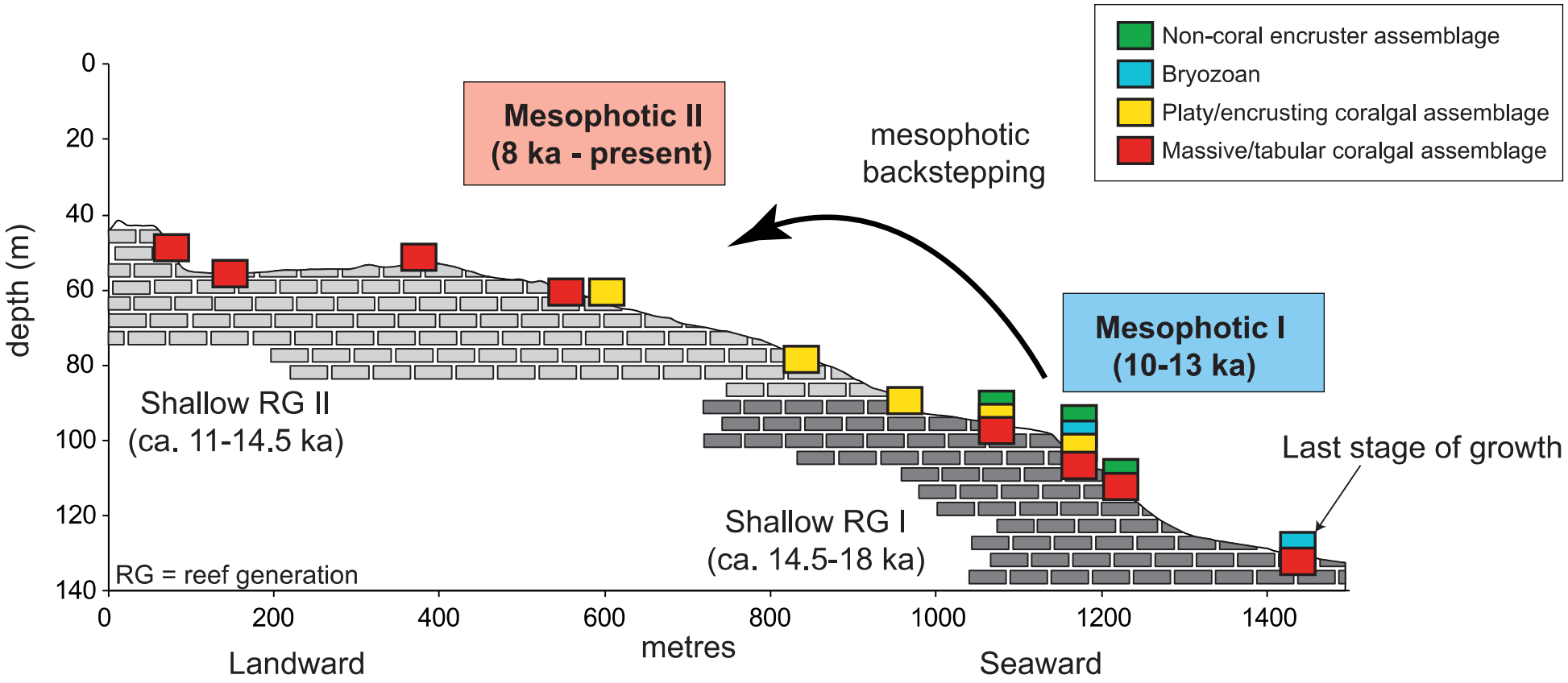

Figure

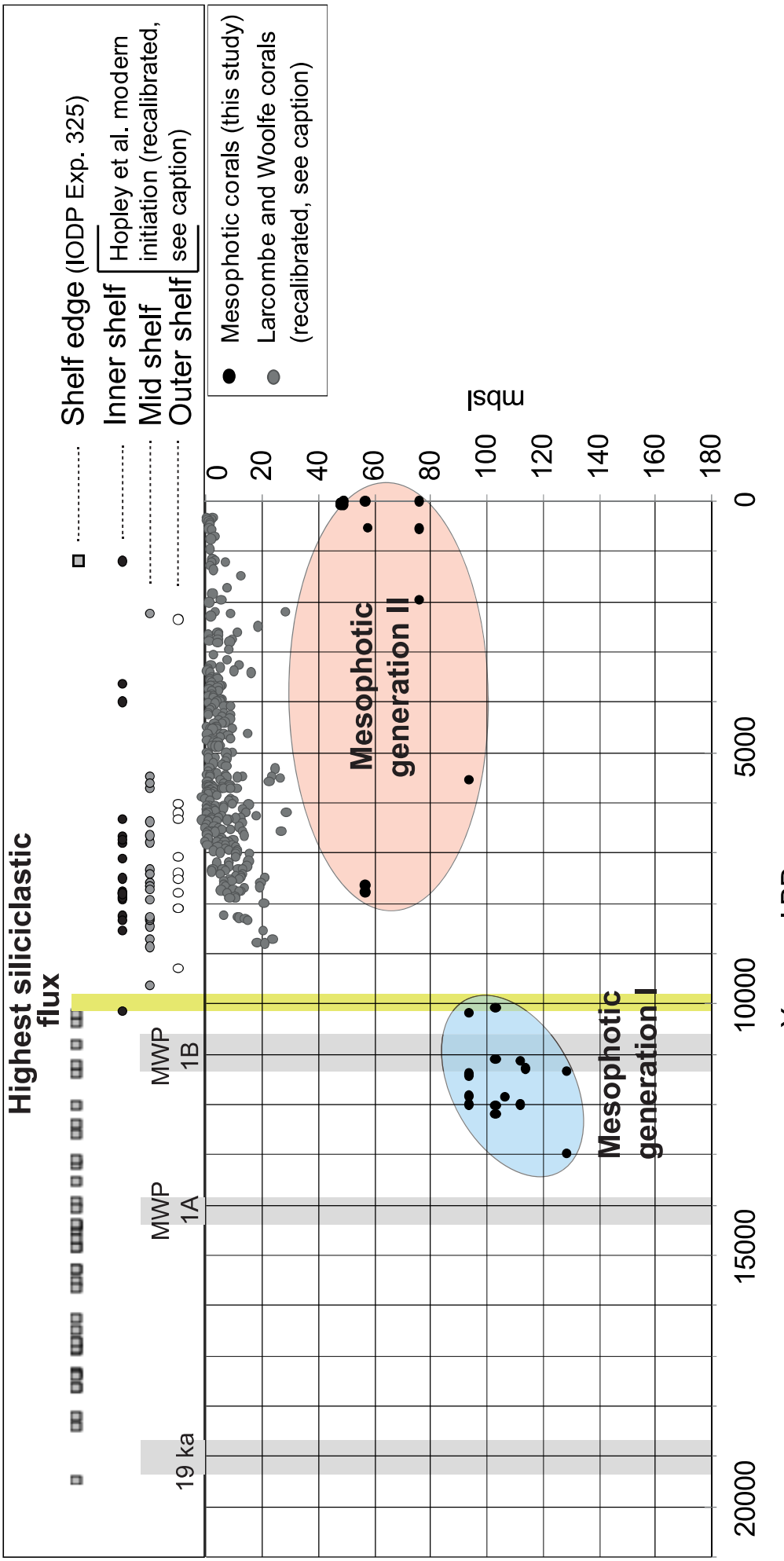

Figure 13. Evolution of fossil GBR mesophotic reefs

Table

Click here to download Table: Table_1_Dredge_location_table.docx

Table 1.

Site	Dredge	Location	Dredged distance (m)	Depth range (m)	Slope range (°)	Morphology of dredged area	Samples
Ribbon Reef	Dr2	-15.3764/145.7966 to -15.3757/145.7967	78	46-50	3.5-17.5	Outer barrier reef	31
	Dr4	-15.4893/145.8191 to -15.4904/145.8188	124	47-51	4.5-27	Outer barrier reef	16
	Dr3	-15.3768/145.7988 to -15.3768/145.7983	54	70-82	4.5-40.5	Shelf break and terrace	134
Noggin Pass	Dr8	-17.1052/146.5723 to -17.1052/146.572	97	53-60	3-27.5	Outer barrier reef	67
	Dr9	-17.0919/146.5663 to -17.0908/146.5658	154	54-61	2-23.5	Outer barrier reef	58
	Dr6	-17.1278/146.5861 to -17.1268/146.5859	133	87-91	4.5-16	Terrace rim	2
	Dr5	-17.1262/146.5871 to -17.1268/146.5872	65	100-102	2-18	Shelf break	3
	Dr11	-17.0923/146.5723 to -17.093/146.573	129	98-108	0.5-31	Upper slope	18
	Dr7	-17.1034/146.5784 to -17.1027/146.578	173	107-120	3.6-18.5	Upper slope	4
	Dr10	-17.0238/146.5445 to -17.0238/146.5778	60	101-124	7.4-13.6	Upper slope	12
Viper Reef	Dr18	-18.8816/148.443 to -18.8822/148.4437	116	57	0.5-1.5	Upper shelf	46
	Dr17	-18.8788/148.4464 to -18.8782/148.4458	80	66-69	1.5-3.5	Upper shelf	47
	Dr16	-18.877/148.4492 to -18.8774/148.4503	121	93-94	3-6.5	Terrace	63
	Dr15	-18.876/148.452 to -18.8765/148.4518	69	101-112	4.5-17	Shelf break	58
	Dr20	-18.8853/148.4859 to -18.8851/148.485	98	104-109	13.5-24	Shelf break	35
	Dr19	-18.8848/148.4865 to -18.8843/148.4854	174	110-114	1.5-17	Upper slope	20
	Dr14	-18.777/148.1983 to -18.7771/148.1963	224	159-173	2.5-32.5	Submarine landslide	5
Hydro. Pass.	Dr21	-19.6948/150.2357 to -19.6797/150.2424	100	52-53	1-8	Outer barrier reef	57
	Dr22	-19.7945/150.235 to -19.7975/150.2427	61	86-92	3-26	Terrace rim	106
	Dr26	-19.787/150.4567 to -19.7866/150.4559	110	103-110	2-20	Shelf break and terrace	12
	Dr25	-19.7842/150.4589 to -19.7839/150.4583	98	126-127	0.5-3	Upper slope ridge	9
	Dr24	-19.7297/150.3587 to -19.7299/150.3575	179	127-133	2.5-13.5	Upper slope	128

Table

Click here to download Table: Table_2_U-series isotopes.docx

Table 2.

Dating ID	Dredge (mbsl)	[^{238}U] (ppm)	2σ	[^{232}Th] (ppb)	2σ	(^{230}Th /^{238}U)	2σ	(^{234}U /^{238}U)	2σ	(^{232}Th /^{238}U)	2σ
D4RR2ia	D4 (47-51)	3.3782	0.0012	20.92	0.14	0.004700	0.000018	1.1466	0.0009	2.03E-03	1.3E-05
D4RR2ib	D4 (47-51)	3.5775	0.0005	10.55	0.02	0.001431	0.000019	1.1454	0.0009	9.65E-04	2.2E-06
D22HP2ia	D22 (86-92)	3.8946	0.0005	12.37	0.08	0.1055	0.0004	1.1419	0.0009	1.04E-03	6.8E-06
D22HP4ia	D22 (86-92)	2.5475	0.0004	0.0670	0.0004	0.1204	0.0004	1.1417	0.0009	8.62E-06	5.7E-08
D22HP13ia*	D22 (86-92)	0.46030	0.00011	2.504	0.016	0.1846	0.0007	1.1330	0.0009	1.78E-03	1.2E-05
D22HP15ia	D22 (86-92)	2.4559	0.0003	2.403	0.016	0.1187	0.0004	1.1402	0.0009	3.20E-04	2.1E-06

*Specimen was a bryozoan, all else were coral.

Table

Click here to download Table: Table_3_Taxonomy all biota.docx

Table 3.

Coral	Coralline and other calcareous algae
Family ACROPORIDAE Undet.[F] *Acropora* sp.[FM] *Montipora* sp.[FM] Family AGARICIIDAE Undet.[FM] *Leptoseris* sp.[M] *Pachyseris speciosa*[FM] *Pavona* sp.[M] Family ALCYONIDAE *Lobophytum* sp.[M] Family FAVIIDAE Undet.[FM] *Cyphastrea* sp.[F] *Cyphastrea chalcidium*[F] *Echinopora* sp.[FM] *Fungia* sp.[M] Family OCULINIDAE *Galaxea* sp.[M] *Galaxea astreata*[FM] *Galaxea paucisepta*[FM] Family POCILLOPORIDAE *Pocillopora* sp.[M] *Seriatopora* sp.[M] Family PORITIDAE Undet.[F] *Goniopora* sp.[F] *Porites* sp.[FM]	Family CORALLINACEAE Sub-family MASTOPHOROIDEAE *Hydrolithon* sp.[M] *Hydrolithon breviclavium*[M] *Hydrolithon reinboldii* (?)[FM(?)] *Hydrolithon rupestre?*[F] *Lithoporella* sp.[FM] *Neogoniolithon fosliei*[M] *Spongites* sp. (?) Sub-family LITHOPHYLLOIDEAE *Lithophyllum* gr. *pustulatum*[FM] *Lithophyllum acrocamptum*[M] *Lithophyllum insipidum*[M] *Lithophyllum cuneatum* *Lithophyllum* sp.[FM] *Paulsilvella* sp.[F] Family HAPALIDIACEAE Sub-family MELOBESIOIDEAE Undet.[FM] *Lithothamnion* sp.[FM] *Lithothamnion muelleri* (?)[M] *Lithothamnion prolifer*[M] *Mesophyllum* sp.[FM] *Mesophyllum funafutiense*[FM] Family SPOROLITHACEAE *Sporolithon* sp.[M] *Sporolithon molle*[M] Family PEYSSONNALIACEAE *Peyssonnelia* sp.[FM]
Bryozoan	**Foraminifera**
Family CELLEPORARIIDAE *Celleporaria* sp.	Family ACERVULINIDAE *Acervulina* sp. *Gypsina* sp.

Table

Click here to download Table: Table_4_Coral_abundance_table_dredge.docx

Table 4.

Site	Dredge	CORAL FAMILY													
		Undet.	Acroporidae			Agariciidae		Favidae			Oculinidae		Poritidae		
			Undet.	*Acropora*	*Montipora*	Undet.	*Pachyseris speciosa*	Undet.	*Cyphastrea chalcidium*	*Echinopora*	*Galaxea*		Undet.	*Porites*	*Goniopora*
											paucisepta	*astreata*			
Ribbon Reef	Dr2	**		***	**	*	*	**	*				*	****	*
	Dr3	****	*		*	**	**	*			*		***	***	
	Dr4	**	*	***	***	*		**						****	
Noggin Pass	Dr7													**	
	Dr8	****	*	*	*	**	**	*		***	*	*		**	*
	Dr9	**			****	*	****	*			*			**	
	Dr11						*							*	
Viper Reef	Dr15	***			*	****	*							**	
	Dr16	*					*							**	
	Dr17	***				**		*						**	
	Dr18	***			***	*	**	***						***	*
	Dr19	**		*	***			**	*					***	
Hydro. Pass.	Dr21	*		*	**	**	*	**			***	**	*	****	
	Dr22	****	*	***	**	*		***	*		*		*	***	
	Dr24	***			*	**	*	*				*	*	***	

Table
Click here to download Table: Table_5_Coralgal_assemblage_table.docx

Table 5.

Assemblage	Characteristics	Modern depths
Massive/tabular	Dominated by massive and tabular (>2 cm thick) corals, especially *Porites*, *Montipora* and *Acropora* with associated encrusting and platy growth forms occurs to Corallines are 1-10 mm thick and diverse. Every coralline observed is present within this depth range, and common genera include *Peyssonnelia*, *Lithothamnion* (L. *muelleri*), *Lithophyllum* (*L. insipidum*) and minor *Hydrolithon* (e.g., *H. reinboldii, H. breviclavum*).	Depths of 60 m or less (Bridge et al., 2010; Bridge et al., 2011a), but when massive Favids are dominant this assemblage can extend to 70 m. These algae are found across a wide variety of water depths from < 40-117 m, but *Lithophyllum* becomes rare below 60 m (Marshall et al., 1998; Lund et al., 2000).
Platy/encrusting	Dominated by thin (< 2 cm) encrusting and platy corals, especially *Porites*, *Montipora* and agaricids associated with thin crusts (≤ 1 mm) of CCA, especially *Sporolithon* and Melobesioids (*Mesophyllum funafutiense*).	Depths of 100 m, but usually less than 80 m. Similar platy corals have been observed across many regions of the shelf to depths of 80 m or more (Harris et al., 1996; Hopley et al., 2007), but coral cover is extremely low at these depths (Bridge et al., 2010; Bridge et al., 2011b). Similar algal crusts are common to depths of at least 117 m. (Harris et al., 1996). Beyond 60 m, *Sporolithon* and *Peyssonnelia* become dominant (Marshall et al., 1998; Lund et al., 2000)
Non-coral encrusting	Thin and encrusting CCA interlaryered primarily with Acervulinid and minor bryozoan.	Depths greater than 100 m within boundstone facies, or 55-70 within the macroid facies (see Table 6 for facies descriptions).

Table
Click here to download Table: Table_6_Facies_descriptions table.docx

Table 6. Bio-litho facies descriptions.

Autochthonous facies		
Facies	**Description**	
Boundstones (BD)	The boundstone facies (Wright, 1992) is composed of multiple layers (2+) of encrusting and binding organisms (e.g., Fig. 7D). Growth hiatuses are indicated by a layer of mud, a new crust (ECA, Acervulinid or bryozoan) or a transition to a new coral taxon. This facies comprises seven sub-facies.	Sub-facies coral (BDc) algal (BDa) coralgal (BDca) foraminiferal (BDf) foraminiferal-algal (BDfa) foraminiferal-coral (BDfc) bryozoan (BDb)
Isolated colonies (IC)	In the case of corals and bryozoans, when a growth hiatus is not identified, the specimen is characterised as an isolated colony. Isolated colonies of corals and bryozoans can reach dimensions of up to 51 cm and 25 cm across their longest axis, respectively.	
Rhodoliths (RH)	Rhodoliths are a type of coated grain (oncoid) that comprises an inner bioclastic nucleus, often a coral or bryozoan fragment, and concentric outer crusts. Rhodoliths are encrusted exclusively by algae. Specimens have an average long-axis length of 6.1 ± 2.4 cm.	
Macroids (MC)	Similar in genesis to a rhodolith, macroids are encrusted predominantly by foraminifera (Acervulinids) with varying additional components, often algal and bryozoan (Fig. 7C). Specimens have an average long-axis length of 8.2 ± 2.1 mm	
Indurated boundstones (IBD)	Indurated boundstones are boundstones that have had most, if not all skeletal pore space and bore traces infilled with peloidal and hemipelagic sediments and lithified. Evidence of the original binding biota may remain in the form of light-coloured intercalated layers (e.g. Fig. 7A) and occasional skeletal preservation, but most often the biota is unidentifiable. The rock itself, as well as any biota, is stained to a dark rusty orange to dark brownish-black colour. Density is relatively very high compared to all other facies.	
Crystalline (CN)	The crystalline facies has no identifiable texture and is highly bored and infilled with unlithified sediments. The original facies cannot be identified and for simplicity only, it is grouped within the autochthonous facies.	
Allochthonous facies		
Grainstones (GR)	Grainstones are mud-free with grains larger than 1 mm, most often comprising skeletal grains and foraminiferal tests.	
Floatstones (FL)	Floatstones are moderately to poorly sorted facies comprising > 10% of grains larger than 2 mm and are matrix-supported. They are composed primarily of the disarticulated plates of the green calcareous algae, *Halimeda,* and associated foraminiferal tests and skeletal grains (Fig. 7B). Bivalves are commonly a primary or secondary component.	
Rudstones (RD)	Rudstones are similar in composition to floatstones, but are differentiated by their grain-supported texture.	
Shellstones (SH)	Shellstones are grain-supported with more than 75% of grains comprising shells (usually bivalve) and often incorporating large coral plates. Grains are often large (cm-size) bivalves cemented together.	
Calcimudstones (CM)	Calcimudstones are rare and contain little if any identifiable biota and are dominated by sandy carbonate mud.	

Table

Click here to download Table: Table_7_Facies and biota by site.docx

Table 7.

Site	Feature	Facies	Age range (ka)	Bioerosion/ Encrustation (%)	CCA thickness	Corals			CCA* and associated sediments	
						Modern/recent	In situ fossil	Reworked fossil	Modern	Fossil
Ribbon Reef	Shelf break (70-82 m)	BDca, BDfc and BDfa with rare MC, IBD and FL	Modern – 2.0	60/80	1-11 mm	*Porites* sp., *Leptoseris* sp., *Fungia* sp.?, *Pachyseris* sp.?, *Montipora* sp.	Massive, platy and encrusting *Porites* sp.; encrusting and platy Favid (undet.[†]), platy *Galaxea paucisepta*; massive *Montipora* sp.	Platy and encrusting Poritid (undet.), encrusting and platy *Porites* sp., encrusting and massive Favid (undet.), platy and tabular *Galaxea paucisepta*, encrusting and platy Agaricid (undet.), encrusting and platy *Pachyseris speciosa*, tabular and platy *Acroporid* (undet.), encrusting *Montipora*, sp.	*Mesophyllum* sp. and thin melobesioid[‡]	*Lithoporella* sp.?, *Mesophyllum funafutiense*, interlayered *Mesophyllum* sp. with *Lithoporella* sp., *Peyssonnelia* sp., thin laminar *Lithothamnion* sp.
	Outer barrier reef (46-51 m)	BD (fc,ca, fa) and IC with rare MC	Modern – ?	55/90	1-10 mm	*Porites* sp., *Acropora* sp., *Montipora* sp.?, *Pachyseris speciosa*, *Pavona* sp.?, *Seriatopora* sp., *Lobophytum* sp., Favid (undet.)	Massive and encrusting *Porites* sp., massive Favid (undet.), columnar *Cyphastrea chalcidium,* encrusting plates and robust branching *Acropora* sp., encrusting *Montipora* sp., encrusting Agaricid (undet.)	Massive and encrusting *Porites* sp., massive *Goniopora* sp.?, massive Favid (undet.), massive *Cyphastrea chalcidium*, encrusting and massive Agaricid (undet.), encrusting plates of *Acropora* sp., encrusting *Montipora* sp.	*Lithothamnion muelleri*?, *Lithothamnion prolifer*, *Mesophyllum* sp., *Peyssonnelia* sp. and thin melobesioid , *Hydrolithon breviclavium*, *Hydrolithon* sp.?, *Lithophyllum cuneatum*, *Lithophyllum acrocamptum*, *Lithophyllum insipidum*, *Lithophyllum* gr. *pustulatum*, *Lithoporella* sp., *Neogonlolithon fosliei*, *Neogoniolithon* sp., *Sporolithon molle*, *Peyssonnelia* sp., vermetid gastropods	

Site	Feature	Facies	Age range (ka)	Bioerosion/ Encrustation (%)	CCA thickness	Corals			CCA* and associated sediments	
						Modern/recent	In situ fossil	Reworked fossil	Modern	Fossil
Noggin Pass	Upper slope (98-120 m)	IBD and FL with rare BDc, IC, RD	10.1-11.8	30/15	1 mm		Encrusting *Porites* sp., encrusting *Pachyseris speciosa*	None	N/A	*Hydrolithon rupestre*?, *Mesophyllum funafutiense*, laminar *Lithothamnion* sp., laminar melobesioid, *Peyssonnelia* sp., *Paulsilvella* sp., *Halimeda* sp., pelagic infilling
	Shelf Break (100-102 m)	IBD and CN	None	65/30			None	None	N/A	N/A
	Terrace rim (87-91 m)	IBD	None	65/40			None	None	N/A	N/A
	Outer barrier reef (53-61 m)	BD (ca, fa, c, f, fc), IC and CN with rare MC, IBD, FL, RD and SH.	Modern – 7.8	60/75	1-3 mm	*Pachyseris* sp., *Montipora* sp., *Echinopora* sp., *Pavona* sp.?, *Leptoseris* sp., *Galaxea astreata*, *Acropora* sp., *Pachyseris speciosa*, *Montipora* sp.	Massive *Porites* sp., encrusting and massive *Montipora* sp., platy *Pachyseris speciosa*	Massive, platy and encrusting *Porites* sp., massive *Goniopora* sp., branching *Echinopora* sp., tabular *Galaxea paucisepta*, platy and massive Agaricid (undet.), platy *Pachyseris speciosa*, platy *Montipora* sp.	*Hydrolithon* sp.?, *Mesophyllum* sp., *Mesophyllum funafutiense,* thin melobesioid	Laminar *Lithothamnion* sp., *Hydrolithon reinboldii* ??, *Lithoporella* sp., *Halimeda* sp.
Viper Reef	Submarine landslide (159- 173 m)	IBD	16.3-14.0	25/40	1 mm	Octocoral (undet.)	None	None	N/A	*Lithoporella* sp., *Peyssonnelia* sp., *Mesophyllum funafutiense*, *Spongites*?, *Lithophyllum* sp.?, peloidal

Site	Feature	Facies	Age range (ka)	Bioerosion/ Encrustation (%)	CCA thickness	Corals			CCA* and associated sediments	
						Modern/recent	In situ fossil	Reworked fossil	Modern	Fossil
										sediments, hemipelagic sediments
	Upper slope (110-114 m)	IBD with rare BD (ca, fc, c), IC and CM	11.1-12.3	50/50	1-3 mm		Encrusting and massive *Porites* sp., encrusting plates of *Acropora* sp., encrusting *Montipora* sp., massive Favid (undet.), massive *Cyphastrea* sp.	None	N/A	N/A
	Shelf break (101-112 m)	IBD, CN and IC with rare BD (c, a, b), FL and SH	6.0-9.5	65/65	1 mm		Encrusting *Porites* sp., platy Agaricid (undet.), platy *Pachyseris speciosa*	Platy *Porites* sp., encrusting and platy Agaricid (undet.)	*Sporolithon* sp. (no sori), *Peyssonnelia* sp., thin melobesioid	N/A
	Terrace (93-94 m)	BD (fa, f) and CN with rare MC, IBD and IC	Modern – 5.5	75/85	1-2 mm		Encrusting *Porites* sp.	Encrusting *Porites* sp., platy *Pachyseris speciosa*	*Lithothamnion muelleri*?, *Mesophyllum* sp., *Sporolithon* sp.	N/A
	Upper shelf (57, 66-69 m)	MC, IC, BD (fc, ca) and CN with rare RH	Modern – ?	70\95	1-2 mm	Favid (undet.), *Porites* sp., Agaricid (undet.), *Montipora* sp.	None	Massive, platy, encrusting corals (undet.), encrusting, massive and platy *Porites* sp., massive Favid (undet.), massive and encrusting Agaricid (undet.), platy *Pachyseris speciosa*, platy and encrusting	*Peyssonnelia* sp., *Lithophyllum* gr. *pustulatum*, *Lithothamnion muelleri*?, thin melobesioid, *Halimeda* sp.	N/A

Site	Feature	Facies	Age range (ka)	Bioerosion/ Encrustation (%)	CCA thickness	Corals			CCA* and associated sediments	
						Modern/recent	In situ fossil	Reworked fossil	Modern	Fossil
								Montipora sp.		
Hydgraphers Passage	Upper slope (127-133 m)	IC, CN, BD (b, c, ca) and FL with rare GR, RD, SH, IBD and CM	10.2-12.0	35/85	1 mm		Massive *Porites* sp., branching octocorals	Massive Poritid (undet.), encrusting and platy *Porites* sp., platy *Montipora* sp., massive Favid (undet.), tabular *Galaxea astreata*, platy Agaricid (undet.), platy *Pachyseris speciosa*	Thin melobesioid	*Lithoporella* sp., *Mesophyllum* sp.?, *Lithophyllum pustulatum*, oyster/bivalve cement
	Upper slope ridge (126-127 m)	Rare IC, RD and CN	10.5-11.2	55/85			None	Branching *Echinopora* sp.	N/A	N/A
	Shelf break (103-110 m)	Rare IBD, IC, FL and CN	None available	45/65			Branching octocoral	Branching octocoral	N/A	N/A
	Terrace rim (86-92 m)	IC, FL, CN, BD (c, ca, b) and RD with rare IBD, CM and GR	10.2-13.1	55/65	1-2 mm		Massive *Montipora* sp., massive Favid (undet.)	Branching, platy and massive corals (undet.), massive, encrusting and platy *Porites* sp., massive Favid (undet.), tabular *Galaxea paucisepta*, massive *Cyphastrea chalcidium*, tabular Acroporid (undet.), encrusting plates and branching *Acropora* sp., platy and massive *Montipora* sp., platy Agaricid (undet.), branching *Pavona maldivensis*?	N/A	*Lithothamnion* sp., *Mesophyllum* sp., laminar melobesioids, *Hydrolithon reinboldii*, *Lithophyllum* sp., *Lithophyllum pustulatum*?, *Halimeda* sp.

Site	Feature	Facies	Age range (ka)	Bioerosion/ Encrustation (%)	CCA thickness	Corals			CCA* and associated sediments	
						Modern/recent	In situ fossil	Reworked fossil	Modern	Fossil
	Outer barrier reef (52-53 m)	IC and BD (ca, c) with rare CN, RH and MC	10.2-12.2	45/90	1-10 mm	*Montipora* sp., *Acropora* sp., *Pachyseris speciosa Galaxea astreata*, *G. paucisepta.*, *Seriatopora* sp.	Platy *Porites* sp.	Columnar Poritid (undet.), platy, massive and encrusting *Porites* sp., massive Favid (undet.), tabular *Galaxea paucisepta*, tabular *Galaxea astreata*, encrusting and massive *Montipora* sp., encrusting Agaricid (undet.), platy *Pachyseris speciosa*	*Mesophyllum* sp., *Lithothamnion muelleri*?, thin melobesioid	*Mesophyllum funafutiense*

*CCA=encrusting coralline algae
†Undet=undetermined
‡Melobesioid=member of the Subfamily Melobesioideae, Family Hapalidiacea.

Table

Click here to download Table: Table_8_Chronology_table.docx

Table 8.

Site	Dredge (depth m)	Facies	Biota within specimen (Bold*=dated)	Context	^{14}C age	Calibrated age	2σ range	Calcite (%)	Dating ID	Paired U-Th ID
Ribbon Reef	D2 (46-50)	BDca	Massive **Favid***	I.S.	370 ±35	30	90-0	0.3	OZL402u1	
					375 ±40	40	0-100	0.2	OZL402u3	
		BDc	Crystalline texture then tabular ***Acropora****	I.S.	490 ±25	90	1-150	0.8	OZL414	
	D3 (70-82)	BDfa	Interlayered CCA and Acervulinids then platy Agaricid, then interlayered **CCA*** and Acervulinids	T	420 ±30	0	0	N/A	OZM203	
		BDfa	Interlayered acervulinids with **algae***	T	935 ±30	530	480-610	N/A	OZM201	
		BDca	Platy *Pachyseris speciosa* then interlayered **CCA*** and Acervulinids	T	955 ±25	540	500- 610	N/A	OZL413	
		BDca	Interlayered platy P*achyseris speciosa* and **CCA***	T	2345 ±35	1950	1860-2070	N/A	OZM202	
	D4 (47-51)	BDca	Massive *Acropora* then thick CCA then interlayered thin ***Porites**** and CCA	T	0 ±0	0	0	N/A	CAM1	
		BDca	Massive Favid then *Porites* then massive unknown coral then *Acropora*, then Acroporid	T	0 ±0	0	0	N/A	CAM2	
		BDca	**Favid*** then *Porites* then Acervulinid and thin *Neogoniolithon*?, *Lithophyllum insipidum*, *Lithothamnion prolifer*, *Peyssonnelia* and *Hydrolithon*?	I.S.	33 ±22	0	N/A	0	UBA-11371	
		BDca	*Peyssonnelia*, *Lithophyllum* gr. *pustulatum*, vermetid grastropods then massive ***Porites**** then *Neogoniolithon* and *Lithophyllum insipidum* interlayered then vermetid gastropods then thick *Acropora* with thick crusts of *Hydrolithon*?	Recently I.S.	474 ±22	70	1-150	0	UBA-11370	D4RR2ia, D4RR2ib
Noggin Pass	D7B (107-118)	BDc	Encrusting ***Porites***(?) then coral(?)	I.S.	10,310 ±60	11,290	11,170-11,440	< 2	OZN367	
	D8 (53-60)	BDca	*Porites* then laminated ***Mesophyllum funafutiense****	T	155 ±25	0	0	N/A	OZL411	
	D9	BDca	Bryozoan then encrusting *Montipora* then interlayered **CCA*** and Acervulinids	Recently I.S.	435 ±25	0	0	N/A	OZL410	

Site	Dredge (depth m)	Facies	Biota within specimen (Bold*=dated)	Context	^{14}C age	Calibrated age	2σ range	Calcite (%)	Dating ID	Paired U-Th ID
	(54-61)	BDca	Indurated sediments then 2 mm CCA then massive *Porites* then CCA then encrusting *Porites* then massive ***Montipora**** then CCA then encrusting *Montipora*	I.S.	7185 ±40	7640	7560-7730	< 2	OZN368	
		BDca	3 mm CCA then massive *Montipora* then **CCA*** then bryozoan then CCA then massive *Montipora* then CCA then encrusting *Porites*	I.S.	7320 ±40	7780	7670-7880	N/A	OZN369	
	D10B (107-118)	BDfa	Basal **CCA*** then thick Acervulinids	I.S.	10,005 ±45	10,990	10,770-11,130	N/A	OZM200	
		BDfa	Very thin **CCA*** then thick Acervulinids then indurated sediments	I.S.	9995 ±50	10,970	10,750-11,130	N/A	OZM205	
	D11A (98-104)	BDca	Coral then thin **CCA***	I.S.	9405 ±40	10,240	10,160-10,360	N/A	OZL405	
		BDfa	Interlayered Acervulinids and **CCA*** then coral then Acervulinids interlayered with *M. funafutiense*, *Peyssonnelia* and laminar *Lithothamnion*	I.S.	9250 ±40	10,080	9910-10,180	N/A	OZM196	
	D11B (98-101)	BDb	**Bryozoan***	I.S.	10,000 ±45	10,980	10,760-11,130	N/A	OZM197	
		RD	Parallel ***Halimeda**** grains with *Paulsilvellla* fragments and thin laminar thalli	T	10,550 ±45	11,780	11,550-11,960	N/A	OZM198	
		FL	Parallel ***Halimeda**** grains	T	10,260 ±60	11,230	11,130-11380	N/A	OZN370	
Viper Reef	D14 (159-173)	BDc	**Octocoral***, branching	I.S.	900 ±35	510	440-570	N/A	OZM190	
		IBD	Laminated ***M. funafutiense, Lithophyllum, Spongites****	I.S.	12,550 ±60	13,980	13,810-14,160	N/A	OZL407u1	
					12,600 ±60	14,040	13,810-14,240	N/A	OZM199	
					13,700 ±60	16,330	15,600-16,760	N/A	OZL407u2	
	D15 (101-112)	IBD	Laminated **CCA***	I.S.	8505 ±45	9120	9000-9260	N/A	OZN373	
		IBD	Thin basal **CCA***	I.S.	8625 ±45	9290	9130-9410	N/A	OZN372	

Site	Dredge (depth m)	Facies	Biota within specimen (Bold*=dated)	Context	^{14}C age	Calibrated age	2σ range	Calcite (%)	Dating ID	Paired U-Th ID
		IBD	**Bryozoan*** within hemipelagic matrix	T	8950 ±60	9610	9470-9800	N/A	OZN371	
		BDa	Laminated **CCA*** then bryozoan	I.S.	10,100 ±70	11,100	10,880-11,220	N/A	OZM181	
		BDc	Indurated sediments then encrusting ***Porites****	I.S.	10,590 ±60	11,840	11,580-12,100	1.5	OZM206	
	D16 (93-94)	MC	**CCA*** then thin Acervulinids then CCA	T	420 ±25	0	0	N/A	OZM193	
		BDfa	Laminated interlayered **CCA*** and Acervulinids	I.S.	440 ±25	0	0	N/A	OZM192	
		BDa	Laminated **CCA***	T	1380 ±35	920	810-1010	N/A	OZM191	
		BDca	Thick laminated **CCA*** then encrusting *Porites* then thick laminated CCA then Acervulinids then *Porites* then interlayered CCA and acervulinids	I.S.	5190 ±40	5540	5450-5630	N/A	OZN374	
	D17 (66-69)	BDfc	Agaricid then Acervulinids then CCA then massive **favid***	T	0 ±0	0	0	0.3	OZM180	
	D19B (110-114)	BDc	Massive ***Cyphastrea****	I.S.	10,620 ±60	11,900	11,630-12,120	0.3	OZL406u3	
					10,640 ±70	11,940	11,630-12,280	0.3	OZL406u2	
					10,820 ±70	12,270	12,020-12,420	0.3	OZL406u1	
		BDc	Indurated sediments then massive *Porites* then *Montipora* then laminated **CCA*** 3mm	I.S.	10,080 ±60	11,090	10,880-11,200	N/A	OZM184	
		BDc	Tabular ***Acropora****, 4 cm thick	I.S.	10,770 ±45	12,190	11,990-12,360	0.5	OZM195	
	D20B (104-109)	IBD	Basal **CCA*** then indurated sediments	I.S.	5620 ±35	6000	5900-6130	N/A	OZN375	
		IBD	Basal **CCA*** then indurated sediments	I.S.	8510 ±45	9130	9000-9270	N/A	OZN376	
		IBD	Basal **CCA*** then indurated sediments	I.S.	8870 ±45	9510	9430-9630	N/A	OZN377	
Hydro. Pass.	D21 (52-53)	BDc	Massive ***Galaxea paucisepta****	T	930 ±35	530	480-610	0.3	OZM185	
	D22 (86-92)	FL	***Halimeda****	T	6790 ±40	7310	7231-7406	N/A	OZN378	
		BDca	*Hydrolithon reinboldii*??, laminar melobesioids then massive ***Montipora****	I.S.	9351 ±35	10,190	10,110-10,250	<2	UBA-11372	D22HP2ia
		BDc	Massive **Favid*** then CCA and microbialite	I.S.	10,220 ±60	11,200	11,110-11,320	<2	OZL404 u3	D22HP15ia

Site	Dredge (depth m)	Facies	Biota within specimen (Bold*=dated)	Context	^{14}C age	Calibrated age	2σ range	Calcite (%)	Dating ID	Paired U-Th ID
					10,403 ±34	11,430	11,260-11,660	<2	UBA-11373,	
					10,480 ±70	11,590	11,300-11,910	0.3	OZL404 u1	
					10,520 ±70	11,680	11,330-11,960	0.6	OZL404 u2	
		BDca	***Lithophyllum pustulatum?, Mesophyllum**** bound to massive *Cyphastrea chalsidium*		9340 ±40	10180	10,090-10,260	N/A	OZL403 u4	
			Lithophyllum pustulatum? Mesophyllum bound to massive ***Cyphastrea chalsidium****	T	10,530 ±70	11,710	11,350-11,990	0.3	OZL403 u2	D22HP4ia
					10,575 ±35	11,830	11,640-12,020	<2	UBA-11373	
					10,680 ±60	12,020	11,740-12,270	0.3	OZL403 u1	
					10,790 ±70	12,220	11,950-12,400	0.4	OZL403 u3	
		BDb	Branching **bryozoan*** with *Lithothamnion*	Recently I.S.	11,664 ±45	13,160	13,070-13,300	N/A	UBA-11374	D22HP13ia
	D24A (127-133)	BDb	**Bryozoan***	T	9335 ±45	10,180	10,040-10,270	N/A	OZN379	
		BDc	Encrusting ***Porites***,	T	10,105 ±40	11,130	11,030-11,200	1.4	OZM194	
		BDc	Platy ***Galaxea astreata****	T	10,670 ±60	12,000	11,730-12,260	1.2	OZM186	
		BDb	**Bryozoan***	T	10,690 ±60	12,040	11,830-12,310	N/A	OZM188	
	D24B (127-130)	BDc	Massive **Favid***	T	10,350 ±60	11,340	11200-11,650	0.3	OZM187	
		FL	Parallel ***Halimeda**** grains	T	10,360 ±50	11,340	11210-11,640	N/A	OZN380	
		BDca	Interlayered massive ***Porites**** with CCA	I.S.	11,490 ±60	12,970	12740-13,120	0.8	OZM189	
	D25A (126-127)	BDb	**Bryozoan***	T	9675 ±50	10,530	10410-10,630	N/A	OZN381	
		BDb	**Bryozoan***	T	10,150 ±50	11,160	11070-11,230	N/A	OZN363	

Table

Click here to download Table: Table_9_UTh_chronology_table.docx

Table 9.

Dating ID	Dredge (mbsl)	Age[a] (ka)	2σ	$(^{234}U/^{238}U)_{initial}$[b]	2σ	$^{230}Th_{initial}$ Corrected Ages[a] $(^{230}Th/^{232}Th)_{initial}$		
						0.6	1.0	1.5
D4RR2ia	D4 (47-51)	0.3905	0.0017	1.1468	0.0009	0.276	0.199	0.103
D4RR2ib*	D4 (47-51)	0.0785	0.0018	1.1455	0.0009	0.026	-0.011	-0.057
D22HP2ia	D22 (86-92)	10.50	0.04	1.1462	0.0009	10.44	10.40	10.35
D22HP4ia	D22 (86-92)	12.08	0.05	1.1467	0.0009	12.08	12.08	12.08
D22HP13ia**	D22 (86-92)	19.29**	0.08	1.1404	0.0009	19.24**	19.17*	19.09**
D22HP15ia	D22 (86-92)	11.92	0.05	1.1451	0.0009	11.90	11.89	11.87

*Replicate of Sample D4RR2ia

**Specimen was a bryozoan, and when compared to AMS age of the same specimen (Table 8), open system behaviour is apparent and therefore the U-Th age is suspect.